QUANTITATIVE WAVELENGTH-RESOLVED FLUORESCENCE DETECTION FOR MICROCHIP CAPILLARY ELECTROPHORESIS

Sebastian Götz

Members of the committee:

Chairman:	prof. dr. ir. J. Huskens	Univ. Twente
Promotor:	prof. dr. U. Karst	Univ. Twente
Members:	prof. dr. ing. D. H. A. Blank	Univ. Twente
	prof. dr. J. T. Andersson	Univ. Münster
	prof. dr. ir. A. van den Berg	Univ. Twente
	prof. dr. T. C. Schmidt	Univ. Duisburg-Essen
	dr. A. H. Velders	Univ. Twente
	dr. G. W. Somsen	Univ. Utrecht

QUANTITATIVE WAVELENGTH-RESOLVED FLUORESCENCE DETECTION FOR MICROCHIP CAPILLARY ELECTROPHORESIS

DISSERTATION

to obtain

the doctor's degree at the University of Twente,

on the authority of the rector magnificus,

prof. dr. W.H.M. Zijm,

on account of the decision of the graduation committee,

to be publicly defended

on Friday, September 1st , 2006 at 13.15 hrs

by

Sebastian Götz

born on July 27th, 1976

in Soest, Germany

The dissertation has been approved by the promotor:

prof. dr. Uwe Karst

Für meine Eltern

Contents

Contents

Contents

Abbreviations

ACN	acetonitrile
ATP	adenosintriphosphate
bp	base pair
BSA	bovine serum albumin
CCD	charge-coupled device
CE	capillary electrophoresis
CID	charge-injection device
CL	chemiluminescence
CZE	capillary zone electrophoresis
DAD	diode-array detector
DMSO	dimethyl sulfoxide
DNA	deoxyribonucleic acid
ECL	electrochemiluminescence
EDTA	ethylenediaminetetraacetic acid
EOF	electroosmotic flow
ESI	electrospray ionization
FITC	fluorescein isothiocyanate
HPLC	high performance liquid chromatography
ITO	indium tin oxide
LC	liquid chromatography
LED	light-emitting diode
LIF	laser-induced fluorescence

Abbreviations

LOD	limit of detection
LOQ	limit of quantification
MAA	mercaptoacetic acid
2-MPA	2-mercaptopropionic acid
MCE	microchip capillary electrophoresis
MCP	microchannel plate
µ-TAS	micro total analysis system
MS	mass spectrometry
NBD-Cl	4-chloro-7-nitrobenzofurazan
Nd:YAG	neodymium-doped yttriumaluminium garnet
OLED	organic light-emitting diode
PAGE	polyacrylamide gel electrophoresis
PDMS	polydimethylsiloxane
PEEK	polyetheretherketone
PMT	photomultiplier tube
PVA	polyvinylalcohol
rhod	rhodamine
RSD	relative standard deviation
SARS	severe acute respiratory syndrome
SBD-F	7-fluorobenzo-2-oxa-1,3-diazole-4-sulfonate
SDS	sodium dodecyl sulfate
TTL	transistor-transistor logic
UV/vis	ultraviolet / visible

Chapter 1

Introduction

1.1 Introduction and scope

Miniaturization has clearly been one of the most obvious trends in the development of new analytical separation systems in recent years. Using microchip separations, the consumption of buffer solution and organic solvents as well as the required amount of sample can be significantly decreased. Separation speed and efficiency can be strongly improved compared with conventional systems. However, the trend to smaller dimensions of microchannels and the ever decreasing sample and detection volume require the development of new high-performance detector set-ups. Laser-induced fluorescence (LIF) combined with photomultiplier tube (PMT) detection provides the lowest limits of detection for microchip separations at the moment, but these highly specialized instruments are generally fixed to one single excitation wavelength and provide only little or no chemical information about the analyte.

Consisting of a fluorescence microscope, a spectrograph and an intensified CCD camera, the newly developed detector described in this thesis follows a

more flexible approach. A lamp-based excitation enables the whole visible spectrum of light to be used for excitation and emission. Dispersing the emitted light in a spectrograph and recording the generated spectra with a CCD camera is a way to increase the amount of information, which can be obtained from the analyte. Comparable to a diode-array detector in UV/vis-spectroscopy, the additional dimension of information enables peak assignment due to fluorescent properties and can help detecting hidden coelutions.

Beginning with the recent developments in microchip detection systems, **chapter 2** will present latest advances in optical detection methods that are well adapted to the high demands of rapid microfluidic separations. The focus is directed to current achievements and interesting applications in fluorescence detection, but chemiluminescence detection and UV/vis-absorbance measurements will be described as well.

The newly developed wavelength-resolved detector together with the microfluidic separation system only consists of components that are commercially available. A detailed description along with the special requirements of each part will be given in **chapter 3**. Furthermore, a rapid on-chip CE separation of three rhodamine dyes will serve as a model system to prove the applicability and performance of the wavelength-resolved detection set-up.

Microchip separations are still not very frequently used for routine analyses, because the inherent problems of miniaturization often result in inferior repeatability compared to more common methods, such as high performance liquid chromatography (HPLC) or desktop capillary electrophoresis (CE). Not many examples regarding the quantitative on-chip determination of real world samples can be found in literature.

In **chapter 4** and **5** the newly developed wavelength-resolved detector is applied to the determination of taurine in energy and sports drinks and the analysis of thiols in consumer products, respectively. The obtained quantitative data will be compared to the results of independent HPLC and CE methods.

General conclusions and future perspectives of using wavelength-resolved detection for microchip capillary electrophoretic separations are discussed in **chapter 6**, which concludes this thesis.

4

Chapter 2

Recent Developments in Optical Detection Methods

for Microchip Separations[‡]

This chapter summarizes features and performance of optical detection systems currently applied to monitor separations on microchip devices. Delivering very high sensitivity and selectivity, fluorescence detection still is the most widely applied method of detection. Instruments utilizing laser-induced fluorescence (LIF) and lamp-based fluorescence, along with the recent applications of light-emitting diodes (LED) as excitation sources are covered in this chapter. As the chemiluminescence detection may be performed using extremely simple devices, which no longer require light sources and optical components for focusing and collimation, interesting approaches utilizing this technique are presented as well. Furthermore current applications of UV/vis absorbance detection for microchip separations, as well as innovative approaches for increased sensitivity are described. This chapter focuses on developments and applications published within the last three years and points out exciting new approaches and their perspectives.

2.1 Introduction

Microchip devices following the μ-TAS (micro total analysis system) approach have continuously been growing much more complex over the recent years [1,2]. The possibility of manipulating smaller and smaller amounts of sample volume combined with faster separations has put great demands on the corresponding detection systems. Researchers in this field are driven by the need to develop ultra-sensitive detectors for fast separations, which deliver as much information about the analyte as possible.

This chapter focuses on recent achievements in optical detection techniques for microfluidic devices and on the more dynamic instruments that are adapted to the detection of rapid separations, in contrast to static detection methods.

Fluorescence detection still is the most widely used optical method for microchip analysis, considering its superior selectivity and sensitivity. Regarding the variety of possible excitation sources, laser-induced fluorescence (LIF) is most easily adapted to the dimensions of microchips. The coherent and low divergence laser beam makes it easy to focus on very small detection volumes and to obtain a very high irradiation resulting in one of the lowest limits of detection among all detection systems. Lamp-based excitation systems represent a less expensive but yet more flexible alternative, regarding the choice of wavelength. Microscope-based detectors using xenon- or mercury-lamps are applied to a variety of different analytical problems with impressive results. The recent advances in the development of

high-output light emitting diodes (LED) are reflected in the growing number of publications using this excitation principle. Their small size and low cost production facilitate the incorporation of LEDs into the microfluidic device.

Optical detection without any need for an excitation source or a complicated optical set-up can be accomplished by means of chemiluminescence (CL) measurements. As no additional light source is required, no background light is generated at all. This results in low limits of detection combined with an excellent selectivity.

The broader application of UV/vis absorbance measurements to separations on microfluidic devices is generally hindered by a low sensitivity due to very short optical pathlengths. However, in recent years a growing interest and further development of this technique regarding sensitivity can be observed.

Presenting current applications and recent developments of the last three years, this part of the thesis focuses on the optical detection methods mentioned above. Electrochemical detection has been extensively reviewed by others [3-5] and is therefore, as mass spectrometric detection [6], not subject of this chapter. Other more general reviews covering earlier results have been published elsewhere [7-9], while Viskari and Landers present a recent overview of unconventional, less common detection strategies [10] in their work.

2.2 Fluorescence Detection

2.2.1 Laser-Induced Fluorescence Detection (LIF)

Along with the miniaturization of separation systems to the microchip format, the separation channels have shrunk to only tens of micrometers in widths and height. The overall reduction of organic solvent, buffer solution and sample amount goes along with an extreme reduction in detection volume. Laser-induced fluorescence detection (LIF) is one of the major detection methods for microchip separations, because it can be adapted best to low concentration / low volume systems.

Recent advances in laser technology produced stable light sources, which cover a strongly increasing wavelength range from the ultraviolet to the infrared region of the electromagnetic spectrum, are relatively inexpensive and can easily be focused onto detection areas in the micrometer scale.

The addition of a pinhole in the focus point along the optical path (confocal-LIF) even allows for 3-dimensional focusing and further reduction of the background signal (scattered light, autofluorescence of microchip material). These very low levels of background signal combined with very sensitive photon detection techniques (photomultiplier tubes (PMT), photon counting systems, charge-coupled devices (CCD)) result in the lowest limits of detection of all microchip detection systems.

The fact that only few compounds exhibit native fluorescence is another reason for the low background signals in LIF, especially in comparison with absorption spectroscopy. On the other hand, labeling with fluorescent markers is required for all non-fluorescent analytes.

Although instruments for microchip LIF, such as the Agilent Bioanalyzer 2100 system are commercially available, most researchers depend on home made LIF detection systems. The Agilent set-up is specialized on RNA / DNA and protein-SDS assays. It has been used for the determination of half-antibody species in immunoglobulin G4 (IgG4) [11,12] and the detection of the *Alicyclobacillus acidoterrestris* bacterium in orange juice [13]. The instrument facilitates to perform bio-assays on primed microchips with limits of detection in the lower µg per ml range. The overall package consisting of sample preparation kit, microchip, detector and adapted software is well suited for a range of routine analyses, but lacks the flexibility and modularity usually required in research set-ups. Hence, the vast majority of the laboratory systems are homemade.

They usually consist of the following basic parts: a laser excitation source, an optical system to focus and collect the light, and a photosensitive detector, generally a photomultiplier tube (PMT).

Two main approaches in the optical systems can be found: The first one (figure 2.1a) uses a lens or an objective to focus the laser onto the microchip channel, typically in an angle of 45° or 37° (Brewster's angle), while the collimation of emission light is performed by an objective perpendicular to the chip plane [14-17].
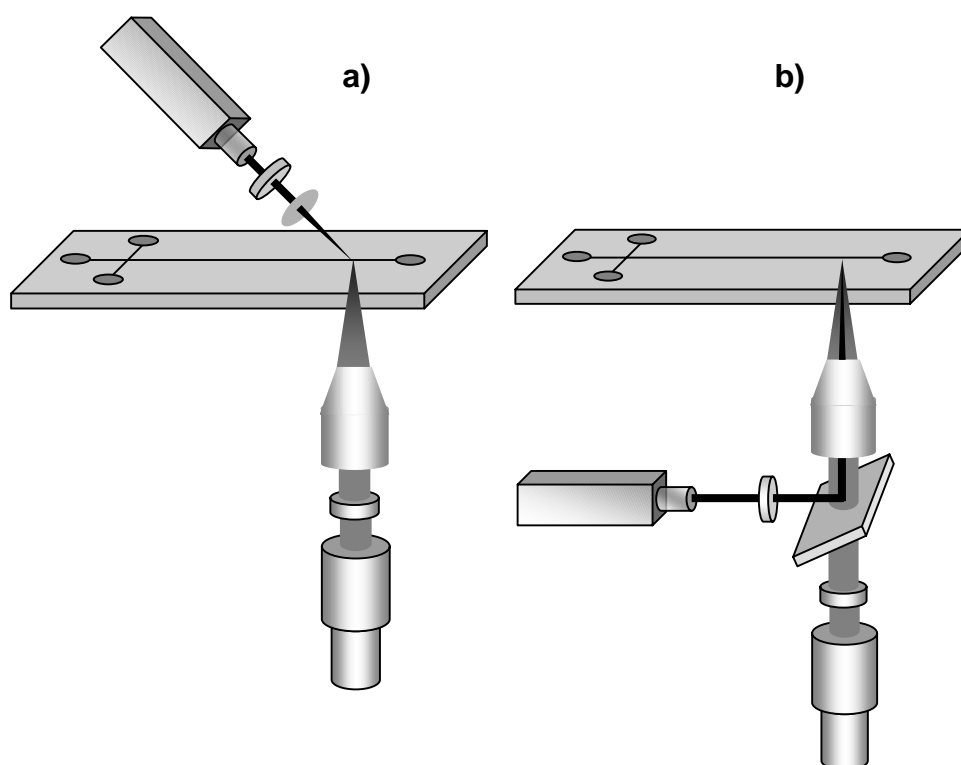
Figure 2.1: a) Common set-up of LIF detection system including laser, excitation filter and focusing lens; emission is collimated by an objective followed by an emission filter and a PMT detector; b) Epifluorescence set-up including wavelength-dependent (dichroic) beam splitter.

The second approach (figure 2.1b) uses the same objective for focusing and collecting the light and a dichroic mirror for wavelength separation [18-25]. For rugged operation and fast optical alignment, the complete optical components of those (epifluorescence) systems are often incorporated into a fluorescence microscope [26-30]. For spatial filtering of the emission and reduction of scattered and background light, most frequently a pinhole is placed into the

focal point along the lightpath. Diameters of those pinholes range from 40 µm to 2 mm.

Lin et al. used a homemade set-up combining a 20 mW laser-diode pumped solid state laser (532 nm), an epifluorescence optics with a 400 µm pinhole and a PMT for bioanalysis. They determined the tumor-associated methylated p16 gene [31] and SARS and hepatitis B virus infections [32] by the analysis of multiplex PCR fragments. Their system had a limit of detection for rhodamine 6G of $6.7 \cdot 10^{-13}$ mol/L with a dynamic range of 3 decades. A 603 bp DNA fragment could be detected at a concentration of 0.2 ng/µL, showing a 40-fold increase in sensitivity compared to slab gel electrophoresis.

The PMT has become the most widely used detector in LIF; it shows excellent sensitivity, a wide dynamic range and a high detection frequency. With the increasing separation speed on microchips, the peak widths grow smaller and smaller. To monitor separations with peak widths below 500 ms, the very high detection frequency provided by photomultiplier tubes is needed.

Liu and co-workers used LIF with PMT detection for a subsecond separation of three flavin metabolites [33]. Without the need of fluorescent labeling the native fluorescence of riboflavin, flavin mononucleotide and flavin-adenine dinucleotide could de detected down to mid nanomolar concentrations.

Qin et al. separated flavin metabolites and developed a very interesting information-rich detector set-up [34]. They used a pulsed nitrogen laser pumping different dye solutions to obtain a tunable laser excitation.

Fluorescence emission was guided to a spectrometer including an intensified CCD-detector. This set-up potentially facilitates wavelength-resolved detection comparable to diode-array detection in UV/vis absorbance measurements. Preliminary results show that, under static conditions, flavin metabolites can be detected in the lower micromolar range, but on-line emission spectra or peak purity plots of dynamic separations have not yet been presented.

Flavin metabolites are one of the rare examples of analytes, which possess native fluorescent properties and can be excited in the visible area of the electromagnetic spectrum. This has made them frequently used model analytes for LIF detection.

However, if excited with UV light, a large number of biological compounds are fluorescent, especially proteins containing tryptophan or tyrosine. Exploiting these native properties is hindered by the fact that the generally used optical components are made of glass, which makes them intransparent for light with a wavelength below 330 nm. Belder et al. built a compact device combining UV filters, a 275 nm dichroic mirror and a UV transparent microscope objective [35]. Fiber-coupled to a 266 nm frequency quadrupled Nd:YAG laser, this cube can be mounted onto the objective holder of a commercially available fluorescence microscope. Keeping in mind that all components in the light path have to be UV-transparent, electrophoretic separations were performed on fused silica microchips. It was possible to detect a separation of proteins with native fluorescence down to a concentration of 12.5 µg/mL (0.9, 0.5 and 0.5 µM for lysozyme, trypsinogen and chymotrypsinogen).

Incorporating optical fibers into the microchip can be one approach to simplify the detection system by minimizing the number of required optical components. Lin and co-workers etched an additional channel into the microchip, in which they introduced an optical fiber coupled to a blue diode-pumped laser (figure 2.2) [36,37]. This channel ended 190 μm away from the separation channel and enabled an excitation without any focusing optical components. Beneath the chip, they attached a 400 μm pinhole, a holographic notch filter (476 nm) and an interference filter (535 nm). The emission light was then directly detected with a PMT from below the chip without any collimating optics. Fluoresceine isothiocyanate (FITC)-labeled epinephrine and dopamine could be detected in a concentration range from $2 \cdot 10^{-4}$ mol/L to $1 \cdot 10^{-7}$ mol/L with a linear response.
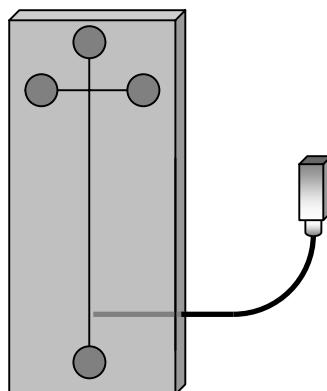
Figure 2.2: Microchip with integrated optical fiber for laser excitation.

A dual wavelength detection approach using integrated optical fibers was presented by Lee et al. [38]. They fabricated a glass / PDMS hybrid chip with two sets of integrated optical fibers facing each other (figure 2.3). Each of the two channels was excited by a separate laser source enabling two different wavelengths (488 and 632.8 nm). The opposite optical fibers were connected to two PMT modules equipped with the appropriate band-pass filters to exclude excitation light. Although no separation was performed, a protein sample plug (BSA) labeled with two different fluorescent dyes (FITC and Cy5) could be observed with the two-wavelength detection set-up. Limits of detection of 200 ppm for labeled BSA are claimed.
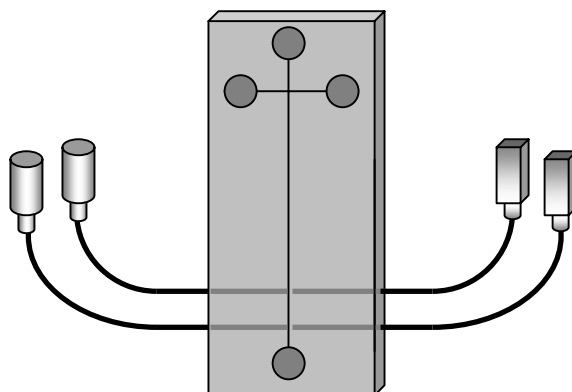
Figure 2.3: Microchip with two sets of integrated optical fibers for laser-induced fluorescence with two-channel PMT detection.

An interesting way of reducing the background signal caused by scattered excitation light is presented by Fang et al. [39]. They use a LIF detection system based on an orthogonal optical arrangement. With an excitation beam perpendicular to the chip, highly sensitive detection was achieved by

collimating the emission light from the microchannel through the sidewall of the chip (figure 2.4).
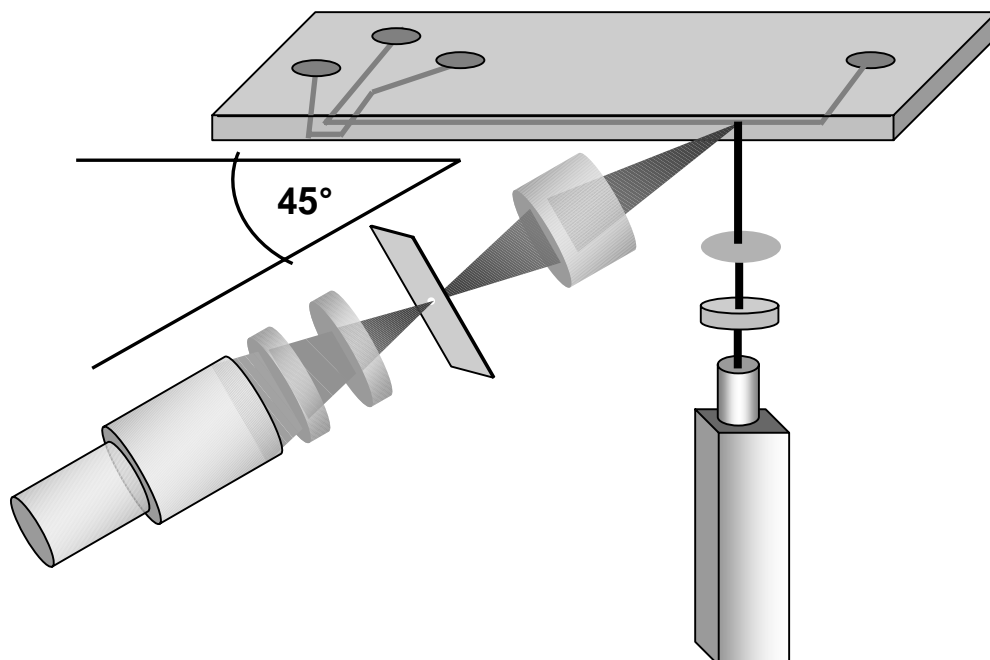
Figure 2.4: Orthogonal LIF set-up with collimation of emission light through the sidewall of the chip.

A special microchip layout was used to bring the separation channel in close proximity of the sidewall (1.5 mm), which was intensively polished to form a highly transparent surface. The emitted light was collimated with a microscope objective and focused onto a 900 μm pinhole. Two filters excluded the remaining excitation light, while the actual detection was performed by a PMT. The amount of scattered light as well as fluorescence emission was found to be dependent on the viewing angle in plane with the chip. Studies of both intensities with regards to the viewing angle revealed the most favorable ratio

between fluorescence signal and scattered light at a collection angle of 45 °, which was then used for further measurements.

The limit of detection for fluorescein was 1.1 pM. The performance of the system was further demonstrated in the separation of FITC-labeled amino acids, which could be achieved at a 100 pM concentrations with RSD values of 3.0 and 3.6 % for FITC-arginine and FITC-phenylalanine, respectively.

An approach for the simultaneous LIF detection of multiple CE separations was proposed by Lin and co-workers [40]. They developed a microchip with four parallel separation channels enabling parallel detection of four different analyte solution. Using a cylindrical lens to form a laser line, a 20 mW solid-state laser (473 nm) was spread along the chip in order to excite all channels at the same time. To conserve the spatial resolution between the different detection points, a CCD-camera was used as a detector. Without the need to reprocess recorded video sequences, they developed a software program that directly showed the appropriate electropherograms of each channel on-line. Four different FITC-labeled amino acids could be separated from their labeling reagent.

The initial unsatisfactory repeatability when comparing the four channels could be improved by the addition of an internal standard to an average of 7.2% RSD, but the use of a 12-bit CCD-camera with a grayscale range from 0 to 4096 made the linearity range of detection very narrow. An application showing the feasibility of the fast screening of chiral selectors was also presented [41].

The goal of lab-on-a-chip applications includes not only the downscaling of the analytical separation system, but the simplification and miniaturization of the detection system as well. Fruetel et al. presented a hand-held CE-LIF device with very impressive abilities [42]. The device utilizes fused-silica microchips to perform simultaneous capillary zone and capillary gel electrophoresis with LIF detection. The instrument shows a modular design, including the separation platform with a multichannel high voltage power supply, a battery pack and the control panel equipped with an LCD-panel for direct evaluation. The separation platform itself incorporates the microchip (2 x 3 cm) with two mirrored separation channels, onto which two 392 nm laser diodes were focused. An aperture and a lens pair gave a nearly Gaussian beam with ~1 mW power delivered to each channel at Brewster's angle (37°). Fluorescence emission was collimated by an aspherical lens and was detected by a PMT after passing a 460 nm long pass filter. The detection of both channels with one single PMT was achieved by asynchronously pulsing the laser diodes at 10 Hz and 50% duty cycle. Software deconvolution separated the data stream into electropherograms corresponding to each channel. Aiming at the detection of biological warfare agents, the device was successfully applied to the separation and detection of fluorescamine-labeled ricin and staphylococcal enterotoxin samples. Additional changes in the design of the instrument, such as the development of a 16-channel high voltage power supply, a new cartridge-based fluid delivery system and a re-designed microchip layout (2 x 2 cm) even further improved the applicability and stability of the system [43]. Providing bi-directional currents up to 100 µA at 5000 V, the high voltage modules enabled real-time current and voltage

monitoring as well. Laser-induced fluorescence detection allowed midpicomolar (10^{-11} M) detection sensitivity of fluorescent dyes and low nanomolar sensitivity for fluorescamine-labeled proteins. It was found that the reproducibility of the migration time could be significantly improved when separations were performed under constant current control (0.5 – 1%) compared to constant voltage control (2 – 8%).

2.2.2 Lamp-Based Fluorescence Detection

As lamp-based excitation is the most widespread method for imaging of biological studies with fluorescence microscopy, those light sources can be very easily applied to the detection of microchip separations by using commercially available microscope set-ups. The common epifluorescence microscope uses condensing optics to collimate and parallelize the lamp-generated light. After reflection by a dichroic mirror, the light is focused with an objective onto the microscope stage. Fluorescence emission is collected by the same objective and usually detected by a PMT after passing the dichroic mirror and an emission filter.

Following LIF detection, lamp-based approaches form the second largest group in optical detection techniques for microchip separations. Two different light sources can be found. High-pressure xenon-arc lamps exhibit a rather homogeneous emission spectrum ranging from the UV up to near infrared

light. Mercury lamps, in contrast, show the typical line spectrum of the excited element. The intensity ratios of the lines and the underlying background are dependent on the pressure in the applied mercury lamp and can result in a quite high radiation output at several fixed wavelengths. If, however, the lines do not match the excitation wavelength of the respective analyte, the flexibility of the broad spectrum of the Xe-lamp can deliver more favorable results.

Several examples of lamp-based excitation using epifluorescence microscopes combined with PMT detection have been reported [44-47] including the detection of a subsecond chiral separation [48] and a fast separation of amino acids in green tea [49]. Chen et al. [50] used this detection method to investigate the capability for quantitative analysis on a flow-through based microchip electrophoresis, while Heineman and co-workers could observe an 160-fold increase in sensitivity by using field-amplified stacking injection for fluorescein derivatives [51].

The highly sensitive instrument developed by Cheng et al. [52] achieved detection limits for FITC-labeled amino acids in the low nanomolar range, comparable to results with laser-induced excitation. The application of a two-channel photon counter behind the preamplifier of the PMT enabled the detection of very weak signals. The limit of detection for FITC was $7 \cdot 10^{-10}$ mol/L. The dynamic range of the system, however, was very narrow (1.5 decades) due to saturation effects in the photon counter.

Although PMTs are by far the most frequently used detectors in this field, being single point detectors, they cannot be used for applications requiring spatial resolution. In contrast, the 2-dimensional chips in charge-coupled devices (CCD) can be sensitive detectors for these quantitative imaging purposes. Han and Singh presented the isoelectric focusing of proteins in short microchannels with SDS-PAGE [53]. A fluorescent protein marker sample (molecular mass range 20,000 – 200,000) was separated in less than 30 s in a channel length shorter than 2 mm. Using an epifluorescence microscope with mercury-lamp excitation, the separation was imaged by a CCD-camera. Protein concentrations from 10 to 100 µmol/L were observed.

Manz and Zhang [54] used a CCD-camera to observe a continuous separation in free-flow electrophoresis (FFE). In FFE, an electric field is applied perpendicular to a hydrodynamically driven stream of analytes. Due to different electrophoretic migration speeds, the analyte streams are diverted from their original flow direction in different angles and are thus separated. The set-up has been successfully applied to the separation of two fluorescent dyes in only 75 ms. The short residence time and small sample flow make the system feasible for the fast monitoring of chemical or biochemical production lines.

A CCD-based approach using the camera not for spatial but rather for spectral resolution was presented by Karst et al. [55]. A xenon-lamp-equipped microscope was used to observe fluorescence emission spectra during rapid microchip CE separations. The emitted light of the analytes was guided to the

entrance slit of a spectrograph, where the light was dispersed. Subsequently the generated spectra were projected onto an intensified CCD-camera. Three rhodamine dyes with complete on-line fluorescence emission spectra were separated in less than 10 seconds. With limits of detection in the midnanomolar range, the system delivered information-rich electropherograms comparable to those of diode-array detectors in UV/vis absorbance measurements, including the possibility of peak assignment due to spectral properties and the detection of hidden co-elution by peak purity plots. The set-up was furthermore successfully applied to the quantitative determination of taurine in beverages [56] and thiols in depilatory cream and cold wave suspensions [57].

2.2.3 Light-Emitting Diode Induced Fluorescence Detection

Light emitting diodes (LED) have recently been introduced as an inexpensive and powerful light source alternative in fluorescence detection. The new generation of LEDs exhibit very high output power covering the whole visible wavelength range and even UV light. LEDs are the most effective light sources available and require only low power driving currents. Combined with their very compact dimensions, they are perfectly suitable for the integration to lab-on-a-chip devices.

However, the half-bandwidth of the emitted light of LEDs often exceeds 20 or 30 nm, which necessitates the implication of additional filters and frequently

generates a higher level of background signal. As the photons in a high output LED are usually generated in an area of a few square millimeters, LEDs are not considered a point source of light. This fact, combined with the divergence of the emitted light, requires a sophisticated collimation and focusing optics to be able to make use of the whole radiation power of the LED.

The commercially available Hitachi SV1100 with a confocal LED detector makes use of a 470 nm LED with a very small radiation area (250 x 250 μm). Using a long pass notch filter and a non-spherical lens, the LED could be used as an excitation source in a common epifluorescence set-up. Focusing of the excitation light could be accomplished down to an area of 120 x 120 μm leading to the general use of microchips with a channel width of 100 μm. After passing the dichroic beamsplitter and an emission filter the emission light is focused by an achromatic lens onto an avalanche photo diode.

The Hitachi SV1100 was used by Dang et al. for the rapid analysis of labeled oligosaccharides [58-60] at low micromolar and submicromolar levels. Compared to a conventional CE-LIF system, much faster separation could be obtained. Similar detection limits for glycosaminoglycans and polysaccharides [61] and the analysis of lipoproteins [62] were found by other groups.

An approach for LED-induced fluorescence detection with integrated LED and optical fiber was presented by Uchiyama and co-workers [63]. Regarding the divergence of light emitted from LEDs, the distance between the diode and the detection area plays a major role. By separating an LED from its epoxy lens, the authors yielded an LED with a flat surface, which was incorporated

22

into the microchip during fabrication. Although due to the extreme proximity no focusing optics had to be used, the broad emission spectra of the used LEDs made the introduction of a thin excitation filter necessary (figure 2.5). An optical fiber was molded into the PDMS chip in a 90° angle to the microchannel.
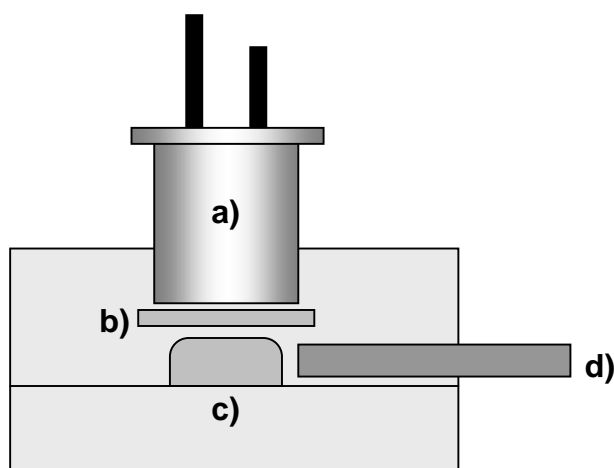
Figure 2.5: Cross section of the microchip with integrated LED (a) and interference filter (b); emission is collected from the separation channel (c) by the integrated optical fiber (d).

While a shorter distance to the separation channel would increase the amount of detected emission light, it was found that if the optical fiber was placed too near, an unwanted deformation of the channel walls occurred. The optimum distance was found to be 100 µm. The emission light was guided through the optical fiber through a band-pass emission filter and was detected by a PMT. Limits of detection could be significantly improved compared to previous results [64]. For fluorescein and rhodamine dyes, they were found to be in the

mid nanomolar range, but the comparison to a microscope-based LIF system showed a 20 times lower sensitivity. This is explained by the fact that all of the laser light is easily focused onto the microchannel, while despite close proximity, only 25% of the emitted light of the LED could be used for detection. With a smaller light-emitting face of the LED combined with optimized driving conditions, further improvements in sensitivity are anticipated.
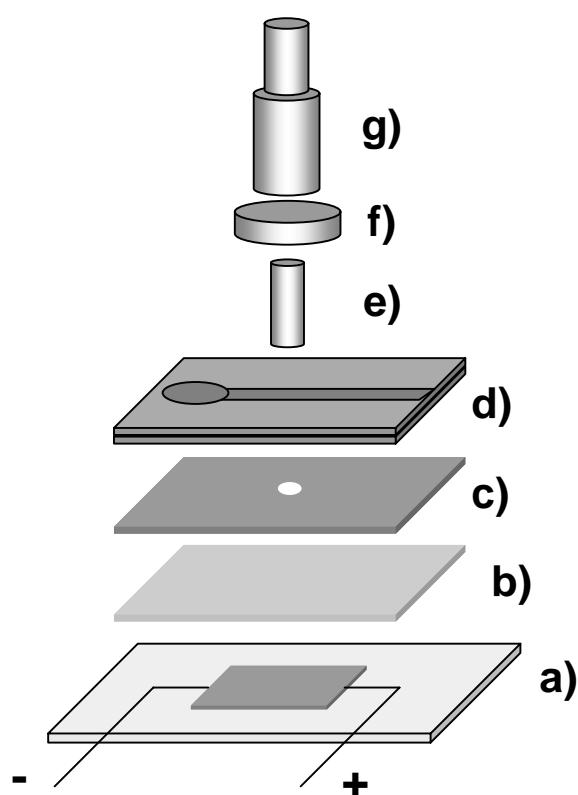
Figure 2.6: Schematic design of the microchip with integrated OLED; a) OLED on glass substrate, b) interference filter, c) pinhole, d) PDMS/glass microchip, e) optical fiber, f) emission filter, g) PMT detector.

Luo et al. [65] followed a similar approach, but made use of organic light emitting diodes (OLED). OLEDs for theses purposes are not frequently used

because they are not yet commercially available and still under development. The big advantage of OLEDs compared to LEDs is their flat film-like shape. This makes it easy to incorporate them into microfluidic devices and to bring them into close proximity to the separation channel. However, the fairly broad emission spectra require the additional application of excitation filters.

In the presented work, a 0.3 mm thin interference filter combined with a 400 μm pinhole is used to yield an effective excitation with the appropriate wavelength (figure 2.6). Detection of the emission light is accomplished by an optical fiber coupled to a PMT. With this system, a detection limit of 3 μmol/L was achieved for the Alexa 532 fluorescent dye. Being several orders of magnitude less sensitive than common LIF detection systems, current drawbacks of OLEDs like low irradiance and light purity have to be solved in order to improve LODs.

2.3 (Electro-)Chemiluminescence Detection

Chemiluminescence (CL) has proven to be a very sensitive and selective detection method in common CE separations. As the light is generated by a chemical reaction, no excitation light source is required and no filter system for background reduction has to be applied. This simplified set-up reveals the obvious attractiveness for the integration of chemiluminescence detection on microchips. However, as the chemiluminescence reagent has to be mixed with the separated analytes before detection, a more complex microchip layout has to be designed. Liu et al. [66] developed several chip layouts (figure 2.7) and evaluated their performance with respect to different chemiluminescence model systems, including the metal-ion catalyzed luminol-peroxide reaction and the dansyl species conjugated peroxalate-peroxide reaction. The separation of Cr(III), Co(II) and Cu(II) ions as well as the chiral recognition of dansyl-phenylalanine enantiomers could be accomplished within one minute with low micromolar and submicromolar limits of detection. The comparison between the different chip layouts showed that the pattern with the Y-shaped cross (figure 2.7 left) was preferred by the luminol-peroxide system, while a V-shaped cross (figure 2.7 right) yielded better results with the peroxalate-peroxide system. The described V-shaped design was further applied to the submicromolar detection of ATP and ATP-conjugated metabolites using a firefly luciferin-luciferase bioluminescence system [67].
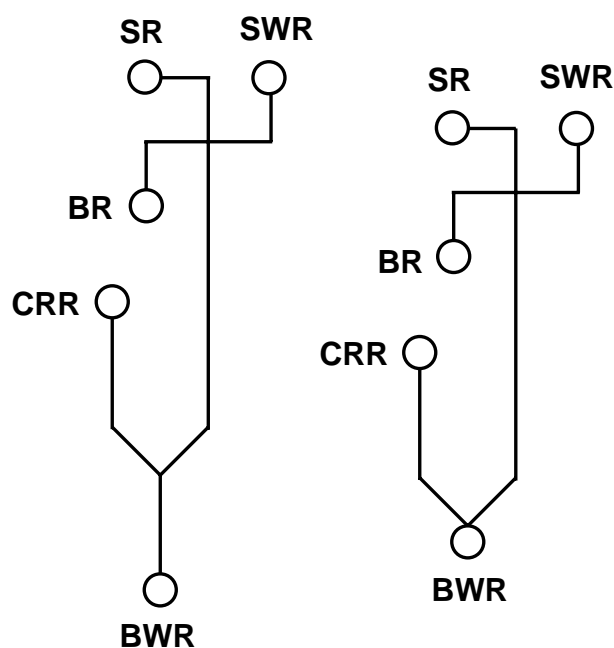
Figure 2.7: Different chip layouts for chemiluminescence detection with sample reservoir (SR), sample waste reservoir (SWR), buffer reservoir (BR), buffer waste reservoir (BWR) and chemiluminescence reagent reservoir (CRR).

While the constant supply of chemiluminescence reagent is very crucial for reproducible detection, it is most frequently delivered by a micropump rather than by electroosmotic flow. Lin et al. used such a system to separate and detect catechol and dopamine [68] as well as dansyl amino acids [69] with limits of detection in the low micromolar range. Ren and Huang [70] developed an extremely simple CL setup. Without the use of any optics or filters, the microchip was directly mounted onto a photomultiplier tube. The back of the chip was made intransparent by the application of black tape, which was only removed in a rectangular window (2 x 3 mm), serving as the detection cell. Applying isoelectric focusing, cytochrome c, myoglobin and

horseradish peroxidase could be separated within 10 minutes with detection limits of $1.2 \cdot 10^{-7}$, $1.6 \cdot 10^{-7}$ and $1.0 \cdot 10^{-10}$ mol/L, respectively.

Wang and co-workers applied an electrochemiluminescence (ECL) detection method to a microchip separation. In ECL, an electroactive compound, in this case tris(2,2'-bipyridyl)ruthenium(II) ($[Ru(bpy)_3]^{2+}$), is oxidized by the application of a voltage to additional electrodes in the separation channel, and subsequently reacts with the analytes under the emission of photons. In the presented work, thin film indium tin oxide (ITO) electrodes were added during the microchip fabrication [71]. The transparency of the ITO material makes them inferior to widely used platinum-based electrodes, because no generated photons are absorbed or deflected. The developed method was applied to the detection of proline and the determination of lincomycin in urine down to a concentration of 9 µmol/L [72], while the additional evaluation of the current at the ITO electrodes facilitated the simultaneous electrochemical detection due catalytic effects of the oxidized $[Ru(bpy)_3]^{3+}$ [73]. They further simplified their system by immobilizing the ruthenium complex on the ITO electrodes [74]. This approach delivered detection limits similar to the earlier described system, but no addition of the complex to the running buffer was required, which drastically reduced the $[Ru(bpy)_3]^{2+}$ consumption.

2.4 Absorbance detection

UV/vis absorbance detection is the most universally used detection method in common chromatographic and electrophoretic separation systems. But despite its very wide field of possible applications, only few examples of absorbance based detection systems for microfluidic separations can be found. The small dimensions of microchip separation channels pose a severe problem for a sensitive and reliable absorbance measurement. The optical pathlength represented by the channel depth is generally shorter than 30 µm.

The presentation of the commercially available Shimadzu MCE system (MCE-2010), equipped with a whole channel UV detection, proved the feasibility of absorbance measurements even in microchip dimensions [75-81]. The Shimadzu detection system incorporates a 1.8 kV high voltage power supply, a deuterium lamp for sample excitation and a linear diode-array (1024 diodes) for a wavelength range of 190-370 nm. In this special design, the diode-array is not used to record absorbance spectra after dispersion of the transmitted light, but is rather aligned along the separation channel to perform whole channel detection (figure 2.8). Specially adapted UV transparent quartz microchips with a separation length of 25 mm are used in this instrument. A narrow optical slit on top of the chip enables the illumination of the whole channel and reduces scattered light detected by the linear diode-array.

Glennon et al. [82] accomplished a fast separation and determination of antimicrobial metabolites from *Pseudomonas fluorensis* F113 and compared

the performance of the MCE separation to a common capillary electrophoretic system. Although the microchip separation (15 seconds) was much faster than the conventional CE separation with a 33 cm capillary (1.9 min), LODs in the low mg/L range were found to be about three times lower than with the common CE set-up.

monochromated UV light

linear diode-array detector
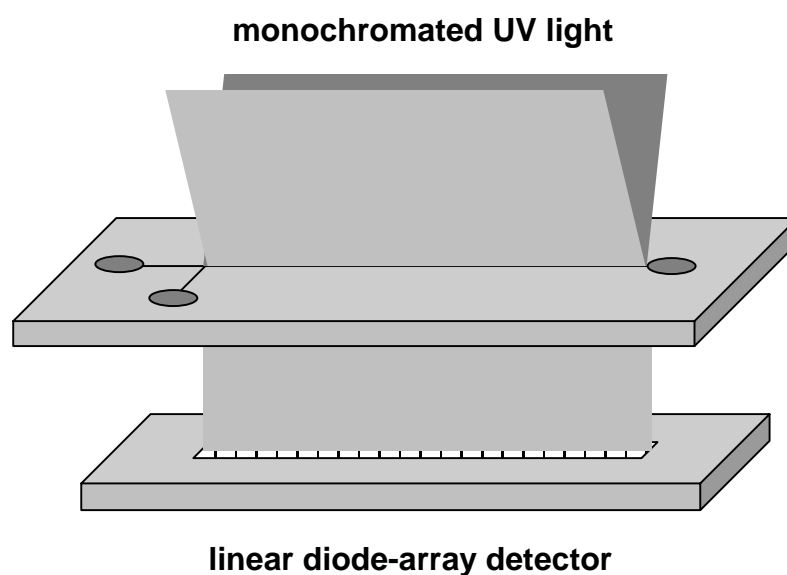
Figure 2.8: Whole channel UV absorbance detection by means of a linear diode array.

Belder and co-workers presented a fast chiral separation using the Shimadzu MCE-2010 [83]. Nineteen basic drugs could be separated from their enantiomeres using several highly-sulfated cyclodextrins as chiral selectors. All separations were performed with analyte concentrations of 2 mg/mL, and were accomplished generally within less than one minute. These limits of detection show that the Shimadzu detector is not designed for trace analysis

but the interesting design of its whole channel detection allows rapid method development, qualitative detection and the determination of samples with high analyte concentration.

A simple fiber optics based UV absorption system was used by Cramer et al. [84] to monitor the capillary electrochromatographic separation of peptides. The separation channel of the microchip was partly filled with a sol-gel immobilized stationary phase (C_4 modified silica, 5 µm particles). UV absorption detection was carried out at the end of the channel without any stationary phase present. Using a XYZ translation stage, the chip was positioned between the ends of two optical fibers facing each other. The top fiber was connected to a deuterium-tungsten light source; the bottom optical fiber collected the transmitted light and guided it into a CCD-array detector. The authors claim that the achieved limit of detection for thiourea (167 µM) could further be improved by noise reduction and a second detection channel for reference monitoring.

Hahn and co-workers [85] used a more complex three-layer chip-design with two integrated optical fibers, a microlens and a pair of slits for extended optical path length absorbance detection (figure 2.9). The slit channels were filled with black ink to absorb any scattered light and ensure that only the transmitted light is collected by the detection fiber. As light coming from an optical fiber is very divergent, both excitation and detection fibers usually have to come very close to yield a sufficient irradiance. To overcome this problem, the authors created a cylindrical microlens in the PDMS material at the end of

the excitation fiber. This way, the divergence could be reduced so strongly that both fibers could still be operated in a distance of over 500 µm.
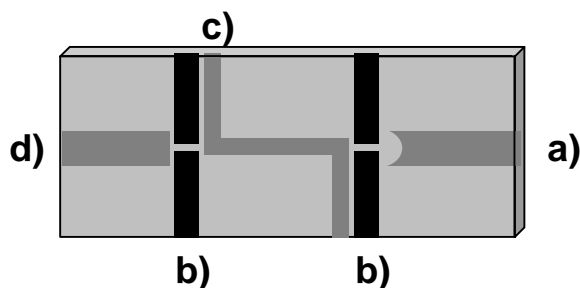
Figure 2.9: Microchip with extended optical pathlength UV absorbance detection; a) channel for excitation fiber was cylindrical lens at the end, b) slit channels, filled with black ink, c) Z-shaped detection cell, d) channel for emission fiber.

This fact was utilized by extending the optical absorbance pathlength. The separation channel (50 µm width) could be redesigned forming a Z-shaped detection cell with an optical path length of 500 µm. As expected from Beer´s law, the sensitivity could be increased almost by a factor of 10. The concentration detection limits for fluorescein, orange II and new coccine were 1.2, 2.9 and 3.5 µM, respectively.

2.5 Conclusions

Considering the number of publications, fluorescence detection is clearly the most widespread optical detection technique for microchip-based electrophoretic separations used within the last three years. While laser-induced fluorescence, with its superior sensitivity, only lacks a certain amount of flexibility regarding the choice of wavelengths, this gap is filled by less expensive lamp-based excitation sources. Depending on the application, the free choice of excitation wavelength frequently seems to compensate for a loss in sensitivity in the order of 2-3 decades. New designs including integrated optical fibers and highly sensitive detectors show that the sensitivity with lamp-based excitation still can be improved.

Light-emitting diodes (LED) are an even more inexpensive alternative for excitation sources. Covering almost the complete electromagnetic spectrum from near UV to infrared, LEDs with higher and higher outputs become available. Although still struggling with high intensity losses during focusing due to the high divergence, next generations of high-output diodes with reduced radiation areas could be able to reach the sensitivity of LIF systems.

Chemiluminescence measurements are a very interesting alternative to fluorescence detections. Lacking the need for any kind of light source or optical components, these systems can be very simple and cost-effective. Although the sensitivity is excellent due to the absence of excitation or stray

light, these chemical systems are only applicable to a rather limited number of applications.

Compared to its importance in common detection systems for conventional liquid phase separations, UV/vis absorbance measurement only play a minor role for microchip applications. Considering Beer´s law, the very short optical pathlengths of microfluidic devices result in a low sensitivity. To minimize this problem, recent publications show the use of integrated optical fibers and extended light path detection cells. Regarding the versatility and ruggedness of a (diode-array) UV/vis detector, they will become more prominent for applications where trace analysis is not the major focus.

2.6 References

1.   Dittrich P S, Tachikawa K, Manz A (2006) Anal Chem 78:3887-3907

2.   Vilkner T, Janasek D, Manz A (2004) Anal Chem 76:3373-3385

3.   Chen G, Lin Y, Wang J (2006) Talanta 68:497-503

4.   Wang J (2005) Electroanalysis 17:1133-1140

5.   Vandaveer W R, Pasas-Farmer S A, Fischer D J, Frankenfeld C N, Lunte S M (2004) Electrophoresis 25:3528-3549

6.   Sung W-C, Makamba H, Chen S-H (2005) Electrophoresis 26:1783-1791

7.   Schwarz M A, Hauser P C (2001) Lab Chip 1:1-6

8.   Morgensen K-B, Klank H, Kutter J P (2004) Electrophoresis 25:3498-3512

9.   Uchiyama K, Nakajima H, Hobo T (2004) Anal Bioanal Chem 379:375-382

10.   Viskari P J, Landers J P (2006) Electrophoresis 27:1797-1810

11.   Vasilyeva E, Woodard J, Taylor F R, Kretschmer M, Fajardo H, Lyubarskaya Y, Kobayashi K, Dingley A, Mhatre R (2004) Electrophoresis 25:3890-3896

12.   Forrer K, Hammer S, Helk B (2004) Anal Biochem 334:81-88

13.   Funes-Huacca M, Regitano L C, Mueller O, Carrilho E (2004) Electrophoresis 25:3860-3864

14.   Ro K W, Hanh J H (2005) Electrophoresis 26:4767-4773

15.   Lee S-H, Cho S I, Lee C-S, Kim B-G, Kim Y-K (2005) Sens Actuators, B 110:164-173

16. Obeid P J, Chrisopoulos T K, Ioannou P C (2004) Electrophoresis 25:922-930

17. Lacher N A, de Rooij N F, Verpoorte E, Lunte S M (2003) J Chromatogr, A 1004:225-235

18. Sandlin Z D, Shou M, Shackman J G, Kennedy R T (2005) Anal Chem 77:7702-7708

19. Qin J, Ye N, Yu L, Liu D, Fung Y, Wang W, Ma X, Lin B (2005) Electrophoresis 26:1155-1162

20. Qin J, Leung F C, Fung Y, Zhu D, Lin B (2005) Anal Bioanal Chem 381:812-819

21. Giordano B C, Jin L, Couch A J, Ferrance J P, Landers J P (2004) Anal Chem 76:4705-4714

22. Jemere A B, Oleschuk R D, Harrison D J (2003) Electrophoresis 24:3018-3025

23. Smith Roddy E, Lapos J A, Ewing A G (2003) J Chromatogr, A 1004:217-224

24. Etoh S, Fujimura T, Hattori R, Kuroki Y (2003) Jpn J Appl Phys, Part 1 42:4093-4097

25. Yang X, Zhang X, Li A, Zhu S, Huang Y (2003) Electrophoresis 24:1451-1457

26. Ling Y-Y, Yin X-F, Fang Z-L (2005) Electrophoresis 26:4759-4766

27. Beard N P, Edel J B, deMello A J (2004) Electrophoresis 25:2363-2373

28. Gao J, Yin X-F, Fang Z-L (2004) Lab Chip 4:47-52

29. Skelley A M, Mathies R A (2003) J Chromatogr, A 1021:191-199

30. Hata K, Kichise Y, Kaneta T, Imasaka T (2003) Anal Chem 75:1765-1786

31. Zhou X-M, Shao S-J, Xu G-D, Zhong R-T, Liu D-Y, Tang J-W, Gao Y-N, Cheng S-J, Lin B-C (2005) J Chromatogr, B 816:145-151

32. Liu D, Zhou X-M, Zhong R, Ye N, Chang G, Xiong W, Mei X, Lin B-C (2006) Talanta 68:616-622

33. Liu B-F, Hisamoto H, Terabe S (2003) J Chromatogr, A 1021:201-207

34. Qin J, Fung Y, Zhu D, Lin B-C (2004) J Chromatogr, A 1027:223-229

35. Schulze P, Ludwig M, Kohler F, Belder D (2005) Anal Chem 77:1325-1329

36. Li H-F, Lin J-M, Su R-G, Uchiyama K, Hobo T (2004) Electrophoresis 25:1907-1915

37. Li H-F, Cai Z-W, Lin J-M (2006) Anal Chim Acta 565:183-189

38. Hsiung S-K, Lin C-H, Lee G-B (2005) Electrophoresis 5:1122-1129

39. Fu J-L, Fang Q, Zhang T, Jin X-H Fang Z-L (2006) Anal Chem 78:3827-3834

40. Shen Z, Liu X, Long Z, Liu D, Ye N, Qin J, Dai Z, Lin B (2006) Electrophoresis 27:1084-1092

41. Gao Y, Shen Z, Wang H, Dai Z, Lin B (2005) Electrophoresis 26:4774-4779

42. Fruetel J, Renzi R F, VanderNoot V A, Stamps J, Horn B A, West J A A, Ferko S, Crocker R, Bailey C G, Arnold D, Wiedenman B, Choi W-Y, Yee D, Shokair I, Hasselbrink E, Paul P, Rakestraw D, Padgen D (2005) Electrophoresis 26:1144-1154

43. Renzi R F, Stamps J, Horn B A, Ferko S, VanderNoot V A, West J A A, Crocker R, Wiedenman B, Yee D, Fruetel J A (2005) Anal Chem 77:435-441

44. Mourzina Y, Steffen A, Kalyagin D, Carius R, Offenhäusser A (2005) Electrophoresis 26:1849-1860

45. Varjo S J O, Ludwig M, Belder D, Riekkola M-L (2004) Electrophoresis 25:1901:1906

46. Wicks D A, Li P C H (2004) Anal Chim Acta 507:107-114

47. Starkey D E, Abdelaziez Y, Ahn C H, Tu J, Anderson L, Wehmeyer K R, Izzo N J, Carr A N, Peters K G, Bao J J, Halsall H B, Heineman W R (2003) Anal Biochem 316:181-191

48. Piehl N, Ludwig M, Belder D (2004) Electrophoresis 25:3848-3852

49. Kato M, Gyoten Y, Sakai-Kato K, Toyo'oka T (2003) J Chromatogr, A 1013:183-189

50. Lin C-C, Chen C-C, Lin C-E, Chen S-H (2004) J Chromatogr, A 1051:69-74

51. Gong M, Wehmeyer K R, Limbach P A, Arias F, Heineman W R (2006) Anal Chem 78:3730-3737

52. Yan Q, Chen R-S, Cheng J-K (2006) Anal Chim Acta 555:246-249

53. Han J, Singh A K (2004) J Chromatogr, A 1049:205-209

54. Zhang C-X, Manz A (2003) Anal Chem 75:5759-5766

55. Götz S, Karst U (2006), submitted to for publication

56. Götz S, Karst U (2006), submitted for publication

57. Revermann T, Götz S, Karst U (2006), submitted for publication

58. Dang F, Kakehi K, Nakajima K, Shinohara Y, Ishikawa M, Kaji N, Tokeshi M, Baba Y (2006) J Chromatogr, A 1109:138-143

59. Dang F, Zhang L, Hagiwara H, Mishina Y, Baba Y (2003) Electrophoresis 24:714-721

60. Dang F, Zhang L, Jabasini M, Kaji N, Baba Y (2003) Anal Chem 75:2433-2439

61. Matsuno Y-K, Kinoshita M, Kakehi K (2005) J Pharm Biomed Anal 37:429-436

62. Ping G, Zhu B, Jabasini M, Xu F, Oka H, Sugihara H, Baba Y (2005) Anal Chem 77:7282-7287

63. Miyaki K, Guo Y, Shimosaka T, Nakagama T, Nakajima H, Uchiyama K (2005) Anal Bioanal Chem 382:810-816

64. Guo Y, Uchiyama K, Nakagama T, Shimosaka T, Hobo T (2005) Electrophoresis 26:1843-1848

65. Yao B, Luo G, Wang L, Gao Y, Lei G, Ren K, Chen L, Wang Y, Hu Y, Qiu Y (2005) Lab Chip 5:1041-1047

66. Liu B-F, Ozaki M, Utsumi Y, Hattori T, Terabe S (2003) Anal Chem 75:36-41

67. Liu B-F, Ozaki M, Hisamoto H, Luo Q, Utsumi Y, Hattori T, Terabe S (2005) Anal Chem 77:573-578

68. Su R, Lin J-M, Qu F, Chen Z, Gao Y, Yamada M (2004) Anal Chim Acta 508:11-15

69. Su R, Lin J-M, Uchiyama K, Yamada M (2004) Talanta 64:1024-1029

70. Huang X, Ren J (2005) Electrophoresis 26:3595-3601

71.   Qiu H, Yan J, Sun X, Liu J, Cao W, Yang X, Wang E (2003) Anal Chem 75:5435-5440

72.   Zhao X, You T, Qiu H, Yan J, Yang X, Wang E (2004) J Chromatogr, B 810:137-142

73.   Qiu H, Yin X-B, Yan J, Zhao X, Yang X, Wang E (2005) Electrophoresis 26:687-693

74.   Du Y, Wei H, Kang J, Yan J, Yin X-B, Yang X, Wang E (2005) Anal Chem 77:7993-7997

75.   Faure K, Loughran M, Glennon J D (2006) Anal Chim Acta 557:130-136

76.   Wakida S-I, Fujimoto K, Nagai H, Miyado T, Shibutani Y, Takeda S (2006) J Chromatogr, A 1109:179-182

77.   Stettler A R, Schwarz M A (2005) J Chromatogr, A 1063:217-225

78.   Xu Z, Nishine T, Arai A, Hirokawa T (2004) Electrophoresis 25:3875-3881

79.   Xu Z, Ando T, Nishine T, Arai A, Hirokawa T (2003) Electrophoresis 24:3821-3827

80.   Xu Z Q, Hirokawa T, Nishine T, Arai A (2003) J Chromatogr, A 990:53-61

81.   Suzuki S, Ishida Y, Arai A, Nakanishi H, Honda S (2003) Electrophoresis 24:3828-3833

82.   Guihen E, Glennon J D (2005) J Chromatogr, A 1071:223-228

83.   Ludwig M, Kohler F, Belder D (2003) Electrophoresis 24:3233-3238

84.   Jinda R, Cramer S M (2004) J Chromatogr, A 1044:277-285

85.	Ro K W, Lim K, Shim B C, Hahn J H (2005) Anal Chem 77:5160-5166

Chapter 3

Wavelength-Resolved Fluorescence Detector for Microchip Capillary Electrophoresis Separations[‡]

A wavelength-resolved fluorescence detector for microchip and capillary separations is developed. It consists of a xenon lamp as flexible excitation source, a fluorescence microscope, a spectrograph with exchangeable gratings (150 and 600 lines per mm) and an intensified CCD-camera.

In contrast to standard LIF-detection systems, this set-up facilitates tuning of excitation and emission wavelengths over the whole visible spectrum of light (350-800 nm). The detector allows to record on-line emission spectra with high repetition rates of up to 60 Hz, which are needed to monitor rapid on-chip separations with peak widths < 0.5 seconds.

In this work, the detector system is applied to the capillary electrophoretic microchip separation of three rhodamines and their impurities. Complete emission spectra of submicromolar solutions are recorded on-line. Comparable with diode-array detection in UV/vis spectroscopy, this detector set-up yields information-rich electropherograms. The additional dimension of information compared to standard fluorescence detection systems enables peak assignment by means of fluorescent properties of the analytes and the immediate detection of co-elutions due to a change of signal ratios at chosen wavelengths (peak purity plots).

43

3.1 Introduction

Capillary electrophoresis (CE) and, in particular, microchip capillary electrophoresis (MCE) suffer from the fact that the most frequently used detection techniques in liquid chromatography (LC), which are based on UV/vis absorbance measurements, require long optical pathways to achieve satisfactory limits of detection as described in Beer´s law. The use of cells with an increased optical pathlength is more difficult than in LC because of the very small detection volumes [1]. Therefore, UV/vis absorbance plays only a minor role for the (ultra)trace analysis using CE and MCE [2].

On the other hand, a technique as photodiode-array-based UV/vis absorbance detection in LC, which provides more characteristic information about the analyte, is required to achieve a high selectivity in MCE. This information could, in principle, be provided by mass spectrometry (MS), but the coupling of MCE with electrospray ionization is not trivial, currently far away from routine application on a large scale and requires very expensive and bulky instrumentation [3].

Fluorescence detection is widely used in MCE due to its very high selectivity and sensitivity. Laser-induced fluorescence (LIF) detection offers the lowest limits of detection, because the highly spatially coherent beam is easily focused onto capillaries or channels used in MCE. Combined with optimized optics, impressive limits of detection for selected fluorophores have been

reported [4,5]. However, little or no chemical and structural information is provided about the analyte.

To increase the degree of information from an MCE separation, this work focuses on the attractive approach to add spectral information to fluorescence detection by dispersing the emitted light, enabling the recording of complete on-line emission spectra. The combination of a fluorescence microscope, a spectrograph and an intensified CCD-camera forms a powerful wavelength-resolved detector set-up, which is easy to use and perfectly adapted to obtain information-rich data sets of rapid microchip separations.

As the detection of four different colors is important in DNA analysis, Mathies et al. developed a four-channel confocal scanner, which they used for DNA sequencing in capillary arrays [6]. The system consists of an arrangement of three dichroic mirrors and four photomultipliers in combination with suitable filter sets, which allow determining four different dyes simultaneously.

In classical CE, but not yet in MCE, other approaches for wavelength-resolved detection have been published. Along with the fast progress in CCD- and CID-based cameras, it was possible to record complete emission spectra during the separation very accurately. Whereas Sweedler et al. [7,8] developed a wavelength-resolved LIF detector with very low limits of detection for fluorescein and bodipy dyes, Blaschke et al. [9] as well as Gooijer et al. [10] used lasers in the UV range to generate native fluorescence of pharmaceuticals and environmental contaminants, respectively. The

wavelength-resolved signal of the array detectors provided additional information on the nature of the analytes after CE separation.

The major drawback of these very powerful systems is their limited flexibility with respect to the choice of the excitation wavelength, which is dependent on the selection of the laser. Furthermore, detection frequencies used in these systems are often insufficient for fast on-chip separations with peak widths below 500 milliseconds.

For these reasons, we have developed a lamp-based approach, which enables the whole visible spectrum of light (350-800 nm) to be used for excitation and emission. In addition, the system is highly flexible with respect to coupling it to rapid MCE and CE separations, which will be shown in the wavelength-resolved detection of the capillary electrophoretic microchip separation of three rhodamines and their impurities.

3.2 Experimental

3.2.1 System Components

An inverse fluorescence microscope (IX-71S1F) from Olympus (Hamburg, Germany) equipped with a 75 W xenon lamp (U-LH75XEAPO) from Olympus was used. A filter cube with components from Chroma (Rockingham, VT, USA) was employed (exciter: HQ470/40x; dichroic: 500DCLP; emitter: HQ510LP) for wavelength selection (figure 3.1).
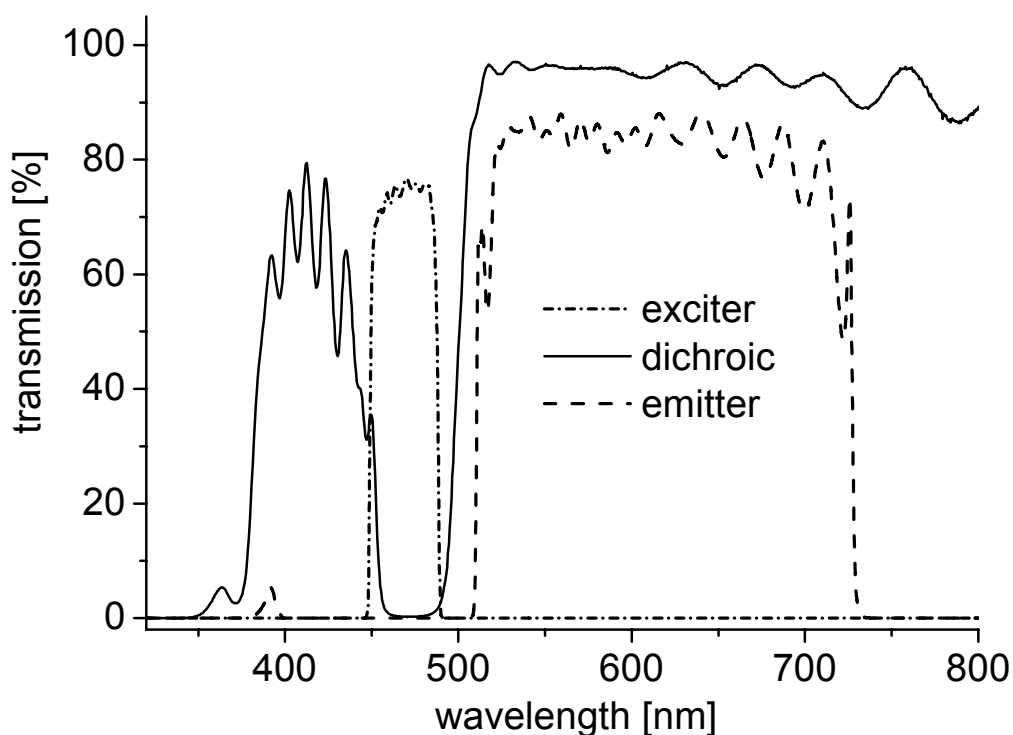

Figure 3.1: Applied filter set consisting of exciter (HQ470/40x), dichroic (500DCLP) and emitter (HQ510LP).

With two Czerny-Turner mirrors and a triple grating-turret, the SpectraPro 308i spectrograph (Acton Research, Acton, MA, USA) provides a focal length of 300 mm. The first grating with 150 grooves per mm projects a wavelength range of about 270 nm onto the CCD-camera, which represents a final theoretical wavelength resolution of 0.52 nm per pixel. The second grating with 600 grooves per mm (0.13 nm per pixel) can be used for higher spectral resolution. The third position of the grating turret is equipped with a mirror for 2D-imaging purposes.

The light intensified CCD-camera PI-Max 512RB from Princeton Instruments (Trenton, NJ, USA) uses a microchannel-plate based amplification system and a front-illuminated Thomson CCD-chip (512 x 512 pixels). The camera was thermoelectrically cooled to -20 °C and combined with a ST133 controller ver.5 (Princeton Instruments). The data was recorded and evaluated with WinSpec/32 software ver. 2.5.12.0 (Princeton Instruments).

A Sony DFW-V500 color camera was used during optimization of separation parameters. The camera was directly mounted to the microscope, thus allowing to record pictures and video sequences.

The high voltage power supply (model ECH-135L) from Micronit (Enschede, The Netherlands) has 8 programmable outputs (0-3000 V) and was additionally equipped with a custom-made trigger output (TTL) to provide a starting signal for the camera.

For pinched injection measurements, model T3550 glass chips from Micronit Microfluididcs (Enschede, The Netherlands) with 10 mm injection and 40 mm separation channel length (figure 3.2) were used (channel cross section: 20 x 50 µm, double-T crossing with 100 µm offset). Separations were performed in an aqueous 40 mM chloroacetate buffer mixed with methanol (buffer:methanol, 2:1) at a pH of 3.0 with a voltage program also shown in figure 3.2.
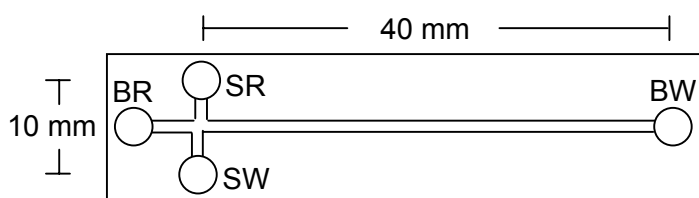
	injection	separation
buffer reservoir (BR)	1300 V	3000 V
sample reservoir (SR)	1900 V	2400 V
buffer waste (BW)	2000 V	0 V
sample waste (SW)	0 V	2400 V

Figure 3.2: Dimensions of the glass microchip and voltages applied to the reservoirs during injection (5 s) and separation (20 s).

3.2.2 Chemicals

All chemicals were purchased from Sigma-Aldrich (Zwijndrecht, The Netherlands) in the highest quality available, except rhodamine 123 (fluoro pure grade), which was purchased from Molecular Probes / Invitrogen (Breda, The Netherlands).

3.3 Results and Discussion

3.3.1 Selection of the system components

Goal of this work is the development of a highly flexible wavelength-resolved fluorescence detector system for MCE and CE. While the literature-known wavelength-resolved detectors (see above) are optimized to achieve the lowest possible limits of detection for a dedicated application, our approach requires the selection of completely different components. The criteria, which should be met by the detector, are the following:

- An excitation wavelength between 350 nm and 600 nm should be possible.

- An emission spectrum of a wavelength range of at least 250 nm has to be recorded.

- To allow coupling to fast separations, a detection frequency of at least 50 Hz is required.

- The limits of detection for fluorophores with good quantum yields should be submicromolar.

For these reasons, the system components described in the Experimental Section were selected. The fluorescence microscope combines highly optimized optics, readily exchangeable filters and mirrors, but is an easy to use and rugged system. The inverse optics leaves much working space above the table to place capillaries or chipholders with connected wires. Centering and focusing of the sample is easily performed as well. Using a xenon lamp in combination with a filter cube instead of a laser facilitates the use of a wide wavelength range (350 – 800 nm) for excitation and emission.

Shorter wavelengths are also generated by the xenon lamp, but cannot be used due to absorption by the glass optics.

As emission spectra of fluorescent analytes in solution are usually quite broad, the dispersion in the spectrograph was predominantly performed by a grating with 150 grooves per mm, which can project a wavelength range of about 270 nm onto the CCD-camera. If a higher resolution is needed, the second grating with 600 grooves per mm can be used. The third position on the turret is equipped with a mirror, which, in combination with the switchable entrance window (12 x 12 mm), enables 2D imaging through the spectrograph without any loss of spatial information. Positioning of the gratings is software controlled and can be changed quickly even during a separation.

The CCD-camera is equipped with a microchannel plate(MCP)-based light amplification system. Combined with the programmable timing generator in the camera controller and a pulsed light source, this system could also be used for time-resolved measurements.

If spatial resolution is not needed, the camera allows binning of arbitrary rectangular areas on the chip. In spectral measurements, for example, every vertical line of 512 pixels (perpendicular to the spectral information) is binned to one single megapixel. This process requires only 512 pixels to be read out at each measuring cycle, which increases the detection speed due to the reduced number of pixels. On the other hand, it also minimizes the readout noise, which is normally generated during the digitization of each single pixel,

resulting in a better signal to noise ratio. Detection frequencies between 30 and 60 Hz were used for the measurements described below.

3.3.2 Detection of a fast on-chip separation

To prove the usefulness of the detector system, it was applied to a fast on-chip electrophoretic separation of three rhodamine dyes, the structures of which are presented in figure 3.3. All of the dyes are excitable with blue light (450 – 490 nm), but show essentially different emission maxima (523 nm for rhod. 123, 550 nm for rhod. 6G and 578 nm for rhod. B). The separation of these model analytes clearly demonstrates how the additional information, regarding the recorded emission spectra, can be used for peak assignment and peak purity plots.
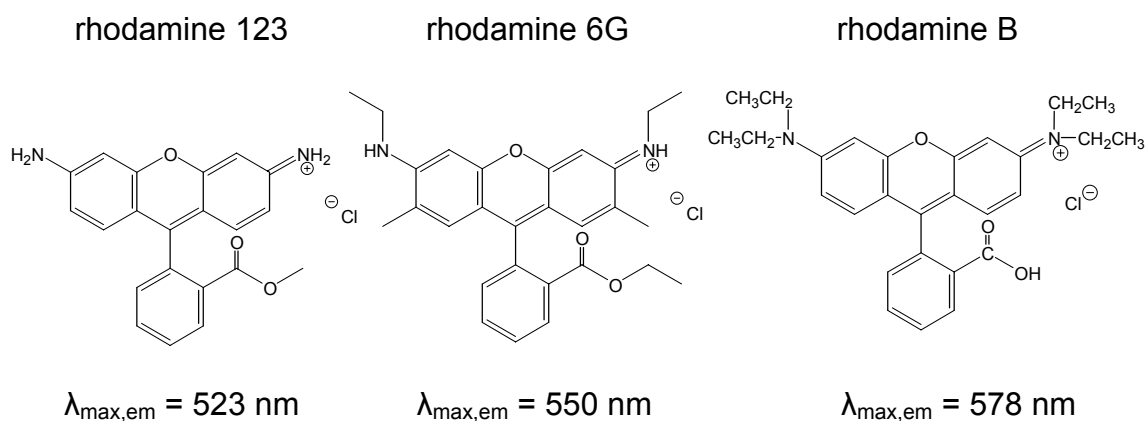
rhodamine 123   rhodamine 6G   rhodamine B

$\lambda_{max,em}$ = 523 nm $\lambda_{max,em}$ = 550 nm $\lambda_{max,em}$ = 578 nm

Figure 3.3: Molecular structures of the three separated rhodamine dyes.

Separations were performed on a commercial CE chip with two orthogonal channels with 20 x 50 µm cross section and a double-T crossing with 100 µm offset. The chip was placed inside a homemade chip holder and covered with two PEEK blocks, which incorporate the four platinum electrodes (0.25 mm diameter), one of them dipping into each of the reservoirs. High voltage cables connect the electrodes to the power supply, which then can be programmed to inject and separate the sample. A programmable TTL trigger was built into the power supply by the manufacturer upon request to allow synchronized starting of the separation system and the detector.

Applying the pinched injection method, the sample plug with an approximate volume of 80 pL is formed within the injection crossing. After 5 seconds, the power supply switches to the higher separation voltage and injects the sample into the separation channel, as recorded with a conventional color CCD camera (figure 3.4). The three rhodamine dyes appear as separated peaks after seven seconds using only the first 3 mm of the available separation distance. Recording the electropherogram with the wavelength-resolved detection system revealed a fourth peak, not detected with the less sensitive color camera. Placing the focus of the objective on different positions along the separation channel enables finding the optimal separation distance. This way, the most rapid separation for a desired resolution of the peaks can be achieved.
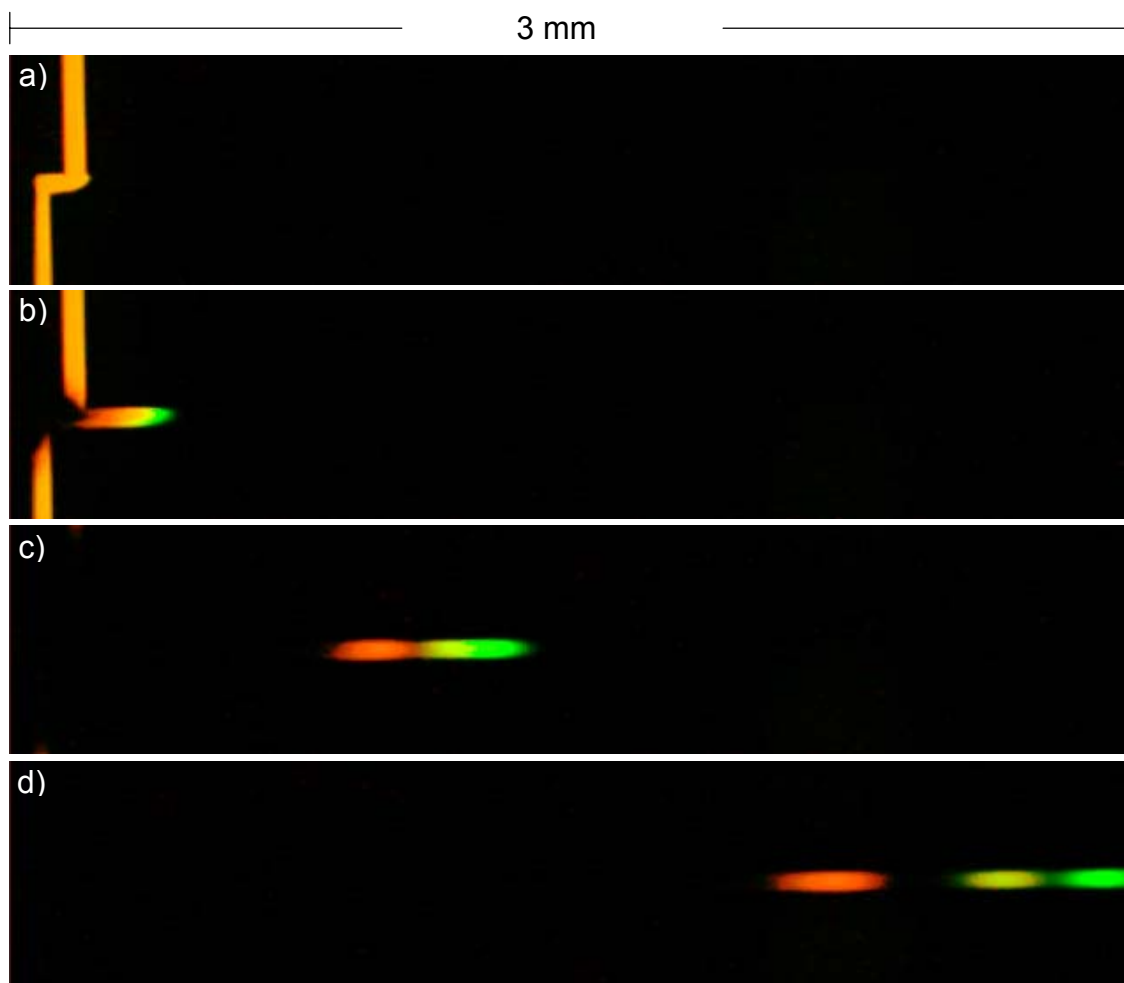
Figure 3.4: Injection and separation of three rhodamine dyes within a distance of 3 mm as recorded by a color camera; a) t = 0 s; stable shape of injection plug is formed; b) t = 0.2 s; switching voltage moves injection plug along separation channel; c) t = 2.5 s; analytes start to separate; d) t = 6 s; the three analytes appear as separated peaks.

Figure 3.5 shows all four peaks with their extracted online-emission spectra, separated within only 10 seconds. The additional small peak was found to be an impurity of rhodamine 123, showing a very similar emission spectrum. This impurity is believed to be rhodamine 110, a green fluorescent dye, with a

molecular structure derived from rhodamine 123. Instead of the ester group it incorporates a carboxylic acid function. This assumption was confirmed by thin-layer chromatography and electrospray ionization mass spectrometry.

Comparable to a diode-array detector in UV/vis spectroscopy, wavelength-resolved fluorescence detection facilitates the application of peak purity measurements. For an existing 3-dimensional dataset, two wavelengths, apparent in all spectra, are selected. With both values meeting a certain threshold, the ratio of the signals is calculated and plotted against time yielding a peak purity diagram shown beneath the electropherogram in figure 3.5. For a pure peak without any underlying spectra, a concentration independent box-shaped signal at the point of the original peak can be seen. Although the third peak shows a higher amount of noise due to the very low signal strength of the impurity, it can be stated that the first three peaks show no sign of underlying spectra. The peak purity plot of the fourth peak, however, clearly indicates a co-elution. The underlying spectrum was found to be caused by rhodamine 19, an impurity of the rhodamine 6G dye. Comparable to the contamination of the green dye above, the structure of rhodamine 19 is derived from rhodamine 6G by ester hydrolysis. The identity of this compound was confirmed by thin-layer chromatography and mass spectrometry.
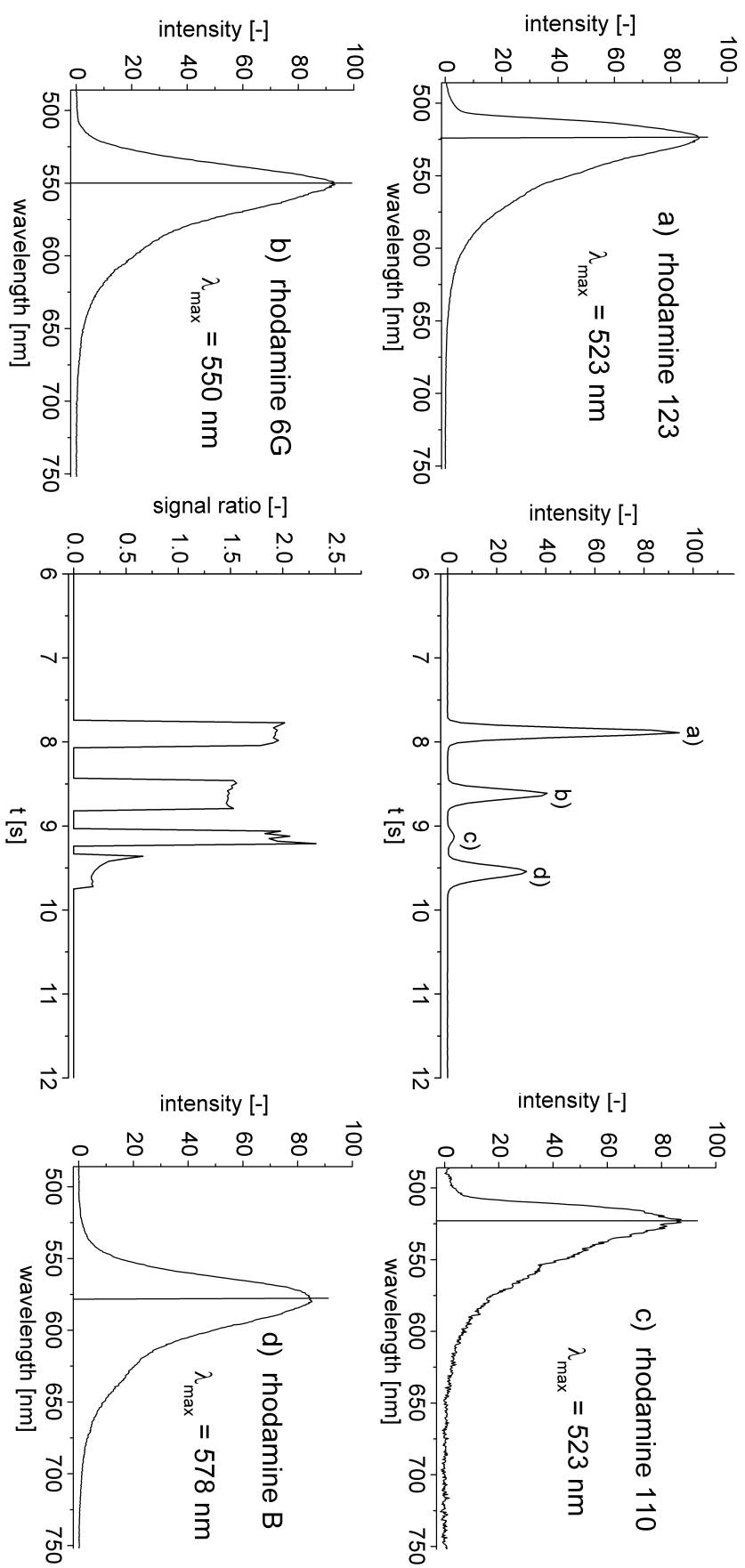
Figure 3.5 Spectrally resolved detection of the on-chip separation of three rhodamines and one impurity in 10 seconds. Extracted online-emission spectra of all analytes are shown. The peak purity plot clearly indicates an underlying spectrum at the fourth peak.

Although the chip was cleaned with 1 M sodium hydroxide solution after every 5 runs, reproducibility problems were observed. Rhodamine B, for example, is known to adsorb to glass surfaces [11], thus changing the surface properties in the channel and leading to an altered EOF. To overcome this problem and to reduce the long chip conditioning times due to excessive etching, the buffer was mixed with methanol (buffer:methanol, 2:1), which slightly decreased the speed of the separation due to higher viscosity, but also reduced the surface interactions to a great extent.

An alternative way of decreasing the adsorption to the channel is applying a dynamic coating of polyvinyl alcohol (PVA) [12,13] to the channel walls. As the addition of methanol showed slightly better results, it was eventually chosen as an organic modifier for further measurements. Calibration curves for all three dyes were recorded, spanning a dynamic range of more than 2.5 decades in each case.

It was found that by using an internal standard, relative standard deviations could be drastically improved. By keeping one of the dyes at a constant concentration, it served as a reference for the other two, hence compensating for deviations in injection volume, migration speed and optical alignment of the detector system. When applying this method of internal standardization the reproducibility of the system could be improved to standard deviations between 0.4 and 7.7% for peak areas with an average of 3.3%. Deviations for migration times ranged from 0.1 to 2.1% with an average value of 0.5% (table 3.1). Limits of detection (S/N = 3) are $1.5 \cdot 10^{-8}$ mol/L for rhodamine 123 and

6G and $3 \cdot 10^{-7}$ mol/L for rhodamine B. Limits of quantification (S/N = 10) mark the lower end of the linear ranges and are $5 \cdot 10^{-8}$ mol/L for rhodamine 123 and 6G and $1 \cdot 10^{-6}$ mol/L for rhodamine B.
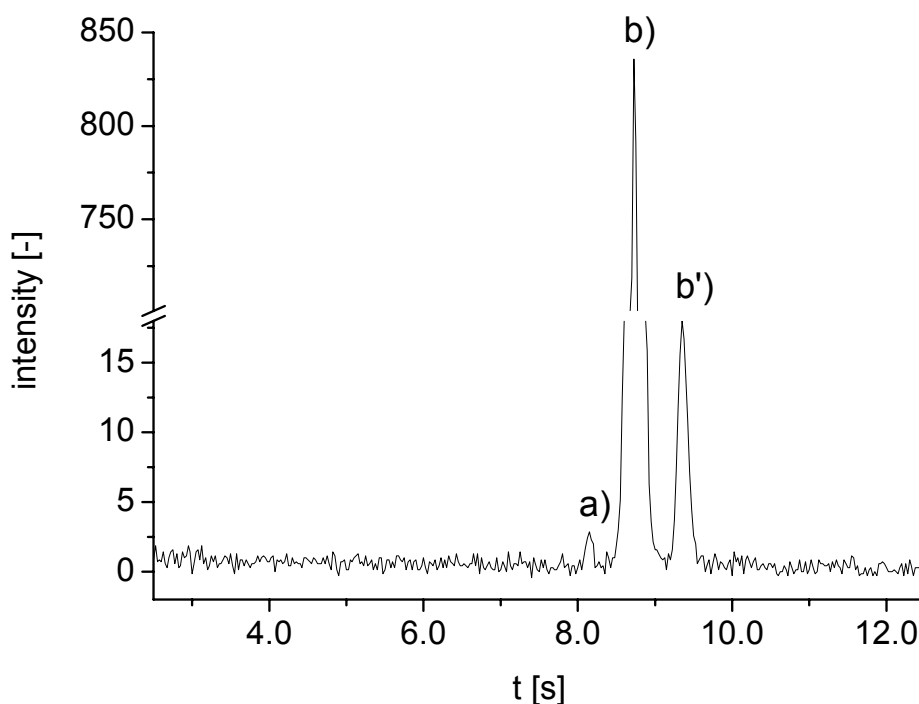
Figure 3.6: Electropherogram of 20 nM rhodamine 123 (a) at its limit of detection (S/N = 3). Rhodamine 6G was used as internal standard (b); b') shows the signal for rhodamine 19, the impurity found in the commercial rhodamine 6G dye.

The efficiency of the separation could be maintained over the whole observed concentration range, even if the mixture contained analytes at very different concentrations. Figure 3.6 shows the electropherogram of rhodamine 123 (peak a) at its limit of detection (S/N = 3). Rhodamine 6G (peak b) was used

as the internal standard and had a concentration of $1 \cdot 10^{-5}$ mol/L. The high concentration ratio of 500 had no influence on the separation. Theoretical plate numbers observed during measurements ranged from 20,000 to 35,000.

Table 3.1: Figures of merit for repeated injection of the rhodamine dyes (N = 3).

	rhodamine123	rhodamine 6G	rhodamine B
LOD [mol/L]	$2 \cdot 10^{-8}$	$2 \cdot 10^{-8}$	$5 \cdot 10^{-7}$
LOQ [mol/L]	$5 \cdot 10^{-8}$	$5 \cdot 10^{-8}$	$1 \cdot 10^{-6}$
avrg σ_{rel}(area) [%]	2.8	1.5	5.5
avrg σ_{rel}(migr. time) [%]	0.2	0.3	1.0
dyn. range [decades]	2.5	2.5	2.5
R^2 for calibration curves	0.9999	0.9999	0.9996

3.4 Conclusions

Combining a fluorescence microscope, a spectrograph and an intensified CCD-camera yields a powerful and flexible fluorescence detector set-up, which is capable of recording complete fluorescence emission spectra during rapid microseparations. The lamp-based excitation enables the complete visible wavelength range to be used, while the CCD-camera allows adapting the detection frequency to the needs of rapid microchip separations.

In this chapter, three rhodamines and one impurity were separated on a CE microchip within 10 seconds. The separation was observed with a detection frequency of 50 Hz. Similar to a diode-array detector in UV/vis-absorbance measurements, the presented system yields information-rich 3-dimensional data sets, thus providing additional qualitative information about the analytes due to their different emission spectra, and enabling detection of hidden co-elution by peak purity measurements.

3.5 References

1.   Salimi-Moosavi H, Jiang Y, Lester L, McKinnon G, Harrison D J (2000) Electrophoresis 21:1291-1299

2.   Schwarz M A, Hauser P C (2001) Lab Chip 1:1-6

3.   Östmann P, Martilla S J, Kotiaho T, Franssila S, Kostiainen R (2004) Anal Chem 76:6659-6664

4.   Ros A, Hellmich W, Duong T, Anselmetti D (2004) J Biotechnol 112:65-72

5.   Chen D Y, Dovichi N J (1994) J Chromatogr, B 657:265-269

6.   Kheterpal I, Scherer J R, Clark S M, Radhakrishnan A, Ju J Y, Ginther C L, Sensabaugh G F, Mathies R A (1996) Electrophoresis 17:1852-1859

7.   Timperman A T, Khatib K, Sweedler J V (1995) Anal Chem 67:139-144

8.   Oldenburg K E, Xiaoyan X, Sweedler J V (1997) J Chromatogr, A 788:173-183

9.   Soetebeer U B, Schierenberg M-O, Schulz H, Hempel G, Andresen P, Blaschke G (2001) Anal Chem 73:2178-2182

10.   Kok S J, Kristenson E M, Gooijer C, Velthorst N H, Brinkman U A T (1997) J Chromatogr, A 771:331-341

11.   Kang J, Yan J, Liu J, Qiu H, Yin X-B, Yang X, Wang E (2005) Talanta 66:1018-1024

12.   Gilges M, Kleemiss M H, Schomburg G (1994) Anal Chem 66:2038-2046

13. Belder D, Deege A, Kohler F, Ludwig M (2002) Electrophoresis 23:3567-3573

Chapter 4

Quantitative On-Chip Determination of Taurine

in Energy and Sports Drinks[‡]

A new method for the quantitative determination of taurine in beverages by microchip electrophoresis was developed. A rapid and simple sample preparation procedure, only including two dilution steps and the addition of the fluorogenic labeling reagent NBD-Cl (4-chloro-7-nitrobenzofurazan), is applied. Using a home-built wavelength-resolved fluorescence detector, the separation and determination of the taurine derivative could be achieved within only 12 seconds, while the additional spectral information was utilized to ensure peak purity. Spanning from 0.1 to 50 mmol/L, the linear dynamic range of the applied method was adapted to the apparent contents in common taurine containing beverages. The smallest detectable amount of the taurine derivative actually injected into the separation channel was as low as 60 amol. The method was successfully validated by an independent liquid chromatographic method.

4.1 Introduction

Since first appearances of lab-on-a-chip applications [1] and the proposal of micro total analysis systems [2], many researchers were fascinated by the apparent advantages of miniaturized separation and detection systems. Ultra short separation times on low-cost disposable devices combined with a strongly reduced amount of sample and organic solvents needed encouraged a large number of research groups to work in this field. Because of the fact that no pumps or pressure-tight connections to the macro world were needed, electrophoretic separations could most easily be adapted to the dimensions of microchips [3] and are still mainly used today. Combined with fluorescence detection, electrophoresis offers very favorable selectivity and sensitivity, rapid separations and very high separation efficiencies. In the following years, many impressive results have been reported, ranging from ultra-trace detection [4] and on-chip derivatization [5] to single cell lysis experiments [6] and ultra fast chiral separations [7]. Despite all the advances made in this area, most of the remarkable work published is of qualitative or semi-quantitative nature. On-chip electrophoresis still suffers from bad reproducibility compared to the results obtained by desktop instrumentation; analytical figures of merit are often extrapolated or calculated from signal-to-noise ratios of single measurements. Only few reports of truly quantitative on-chip determinations with real samples can be found in literature. Inorganic ions, such as nitrite in water [8], calcium in urine [9] and lithium in blood [10] as well as a few more complex analytes, e.g. levoglucosan in aerosols [11], thiols in nerve agent degradation products [12] and homocysteine in plasma

[13] have been determined. Many problems associated with miniaturized separation and detection systems, like pH changes due to electrolysis [14-16], analyte surface interactions [17] and temperature effects [18], have already been addressed and often solved, but mostly in a way not suited for routine analysis.

Taurine (2-aminoethanesulfonic acid) is a semi-essential amino acid, which is abundant in high concentrations in many tissues and body fluids. Although it is not incorporated into proteins, taurine in its free form is associated with a vast variety of physiological functions, such as antioxidation activity [19], neuromodulation, membrane stabilization [20] and modulation of intracellular calcium levels [21]. While in a healthy state, intercellular taurine levels are strictly controlled, altered concentrations in plasma and urine have been associated with a variety of diseases including epilepsy [22], myocardial infarction [23] and cancer [24]. Regarding the importance of taurine in retinal development, reproduction and development it has been added to infant formula as well as to parental solutions [25]. In recent years, with the propagation of energy and sports drinks, the normal daily uptake of taurine could easily be exceeded by a factor of 100. Although animal studies have not indicated toxic effects of taurine, the need for a rapid and easy method of taurine determination in food and beverages for quality assurance and product control purposes has become more important.

While taurine can be detected directly by means of pulsed amperometric detection [26], the most frequently used method for taurine determination is

the HPLC separation with subsequent UV/vis or fluorescence detection [27]. The required derivatization reagents include *o*-phthalaldehyde [28], 2,4-dinitrofluorobenzene [29] and fluorescamine [30,31]. In recent years, alternative separation methods like ion-exchange chromatography [32] and particularly capillary electrophoresis [33] became more prominent.

In this chapter, the quantitative determination of taurine in sports drinks and other taurine containing beverages by means of a very rapid on-chip CE separation and wavelength-resolved fluorescence detection is presented. A fast and easy way of receiving reliable data with reproducibility comparable to other established methods is described.

4.2 Experimental

Taurine standard solutions were derived by dilution from a freshly prepared 100 mM stock solution of taurine in demineralized water. Real samples were diluted 3 to 10 fold, depending on their concentration of acidity regulators to ensure the proper pH during derivatization and yield final taurine concentrations in the linear range of the detector.

Taurine standard or real sample solutions (30 µL) were mixed with 30 µL of buffer (700 mM aqueous borate buffer, pH 9.3) spiked with a 30 mM concentration of 6-aminohexanoic acid as internal standard. After addition of 60 µL of a 200 mM solution of 4-chloro-7-nitrobenzofurazan (NBD-Cl) in acetonitrile, the mixture was shaken and incubated at 45 °C for 30 minutes. Subsequently, the reaction solution was diluted 10 fold with running buffer and then applied to the reservoir of the microchip and injected and separated in triplicate.

Separations were performed on glass microchips (model T3550) from Micronit (Enschede, The Netherlands) with an orthogonal channel design (10 mm x 40 mm) and a channel cross section of 20 x 50 µm. The chips incorporate a double-T crossing with 100 µm offset.

The high voltage power supply (model ECH-135L) from Micronit Microfluidics (Enschede, The Netherlands) comprises 8 programmable outputs (0-3000 V)

and was additionally equipped with a custom-made trigger output (TTL) to provide a starting signal to the camera.

The chip was flushed once every three runs with running buffer (50 mM borate buffer, pH 9.3). The voltages applied during analysis are shown in figure 4.1.
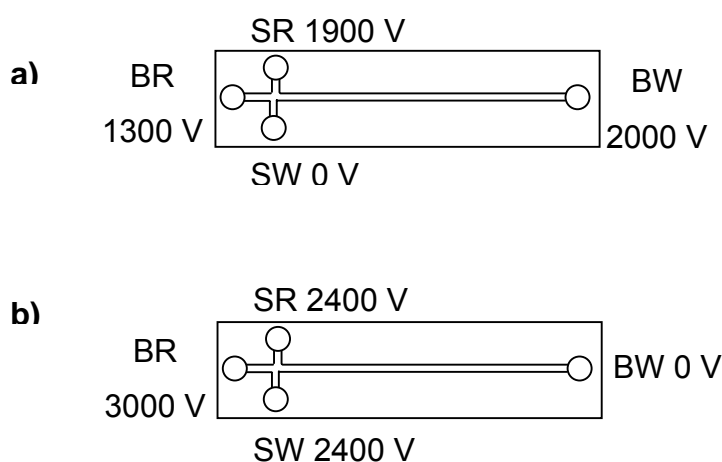
a)

SR 1900 V

BR 1300 V

BW 2000 V

SW 0 V

b)

SR 2400 V

BR 3000 V

BW 0 V

SW 2400 V

Figure 4.1: Voltage program for pinched injection (buffer reservoir (BR), buffer waste (BW), sample reservoir (SR) and sample waste (SW)); a) injection (5 sec) and b) separation (20 sec).

Separations were observed with a wavelength-resolved fluorescence detector consisting of a fluorescence microscope, a spectrograph and a CCD-camera [34]. An inverse fluorescence microscope (IX-71S1F) from Olympus (Hamburg, Germany) equipped with a xenon burner (U-LH75XEAPO) from Olympus was used. A filter cube with components from Chroma

(Rockingham, VT, USA) was employed (exciter: HQ470/40x; dichroic: 500DCLP; emitter: HQ510LP) for wavelength selection.

The triple grating turret in the spectrograph SpectraPro 308i (Acton Research, Acton, MA, USA) was provided with a 150 grooves per mm (gr/mm) grating for standard measurements, a 600 gr/mm grating for high resolution spectra and a mirror for imaging.

The light intensified CCD-camera PI-Max 512RB from Princeton Instruments (Trenton, NJ, USA) was combined with a ST133 controller ver.5 (Princeton Instruments). The data was recorded and evaluated with WinSpec/32 software ver. 2.5.12.0 (Princeton Instruments).

For validation purposes, the analysis was also performed on an HPLC system with fluorescence detection. Liquid chromatographic separations and the detection were performed on the following system (all components from Shimadzu, Duisburg, Germany): two LC-10AS pumps, degasser GT-154, RF-10AXL fluorescence detector, SIL-10A autosampler, software Class LC-10 version 1.6 and CBM-10A controller unit. The injection volume was 10 µL. A Prontosil 120-3-C18 column (Bischoff Chromatography, Leonberg, Germany) was used; particle size 3 µm, pore size 120 Å; column dimensions 150 mm x 4.6 mm.

To ensure a sufficient retention of the highly polar analytes, a gradient of an acidic buffer (10 mM acetate, pH 5) and acetonitrile with a flow of 1 mL/min has been used (table 4.1). Sample preparation was performed analogous to the on-chip separation, except for the fact that the reaction solution was diluted by a factor of 100 with water prior to injection.

Table 4.1: Binary HPLC gradient; A) aqueous buffer (10 mmol pH 5.5); B) acetonitrile.

	0 min	10 min	15 min	19 min	23 min	25 min
A	90 %	80 %	60 %	10 %	90 %	stop
B	10 %	20 %	40 %	90 %	10 %	stop

4.3 Results and discussion

The goal of this work is the quantitative determination of taurine in energy drinks and other taurine containing beverages by means of a microchip capillary electrophoretic separation with wavelength-resolved fluorescence detection. As taurine itself is neither fluorescent nor UV-active, it has to be labeled. In this work, we use 4-chloro-7-nitrobenzofurazan (NBD-Cl) as a reagent. The non-fluorescent NBD-Cl binds to amine functions at elevated pH values and forms the respective NBD derivatives, which show strong fluorescence (figure 4.2).
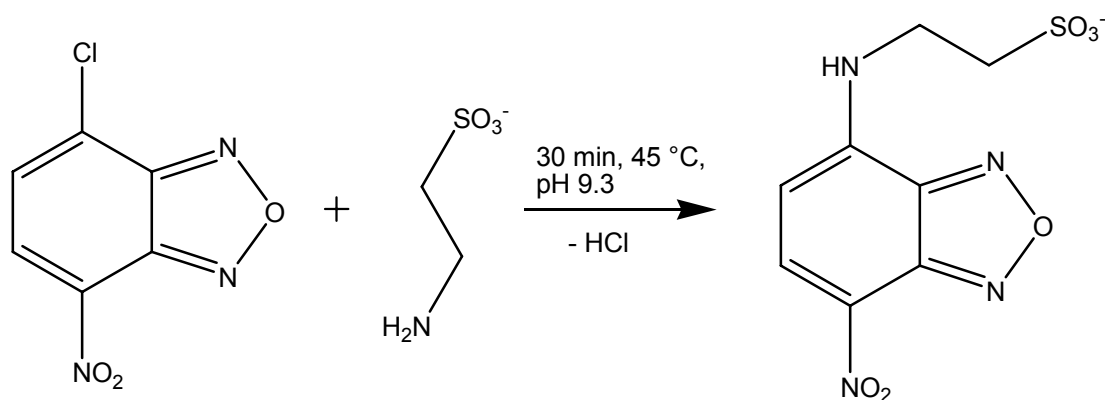

Figure 4.2: Derivatization of taurine with NBD-Cl under basic conditions.

To improve the reproducibility of the quantitative measurements, all standard solutions and samples were spiked with 6-aminohexanoic acid as an internal standard. The use of the internal standard helps to compensate for fluctuations in the amount of injected sample, in reaction speed during derivatization, in the optical alignment of the detector and in slight changes of migration speed.
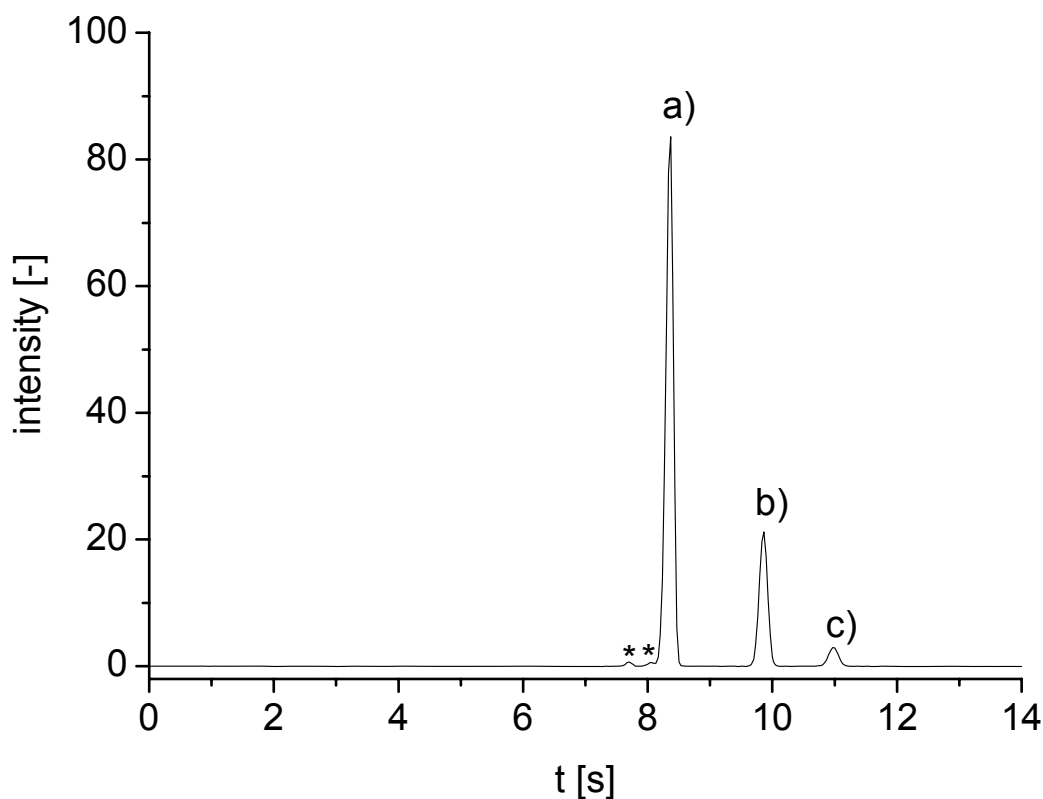
Figure 4.3: Electropherogram of a taurine standard solution (10 mM); a) internal standard, b) taurine derivative, c) hydrolysis product; * mark unidentified peaks.

After dilution, the reaction mixture is directly filled into the sample reservoir of the microchip and injected into the separation channel. The electropherogram of a derivatized taurine standard is shown in figure 4.3. The electropherogram shows three major peaks with peak a) being the internal standard and b) being the taurine derivative. Peak c) is a hydrolysis product of the NBD-Cl reagent, where the chloride function was exchanged with a hydroxy ion. Two very small peaks caused by yet unidentified side products of the derivatization in front of peak a) can also be seen (*). They are apparent in all separations,

but do not interfere with the quantification. The complete separation is accomplished within 12 seconds.

The applied wavelength-resolved fluorescence detector set-up consists of a fluorescence microscope, a spectrograph and a CCD-camera and yields information-rich electropherograms comparable to a diode-array detector in UV/vis spectroscopy. Figure 4.4 shows the extracted emission spectra of the three major peaks. Compared to the spectrum of the internal standard a) with an emission maximum of 551 nm, the taurine derivative b) shows a slight shift of the maximum to 548 nm and a more expressed shoulder on the left side of the curve. Even though the fluorescence in both cases is generated by the same NBD-backbone and the two molecules are very similar, subtle differences in their fluorescent properties can be detected. The third spectrum of the hydroxy derivative shows an even stronger shift of the emission maximum to 573 nm. Using the additional spectral dimension of the recorded data, possible coelutions during the separation can easily be detected by means of a peak purity plot. For this purpose, two wavelengths apparent in all observed spectra are selected (545 and 605 nm). If both measured intensities exceed a previously defined threshold value, the ratio between them is calculated and plotted (fig. 4.4).

A clean peak is then observed as a concentration independent box-shaped peak at the point of time of the original peak and the height of the calculated wavelength ratio. A co-elution would show up as a strong change of ratio during one peak [34], but was not observed in these separations.
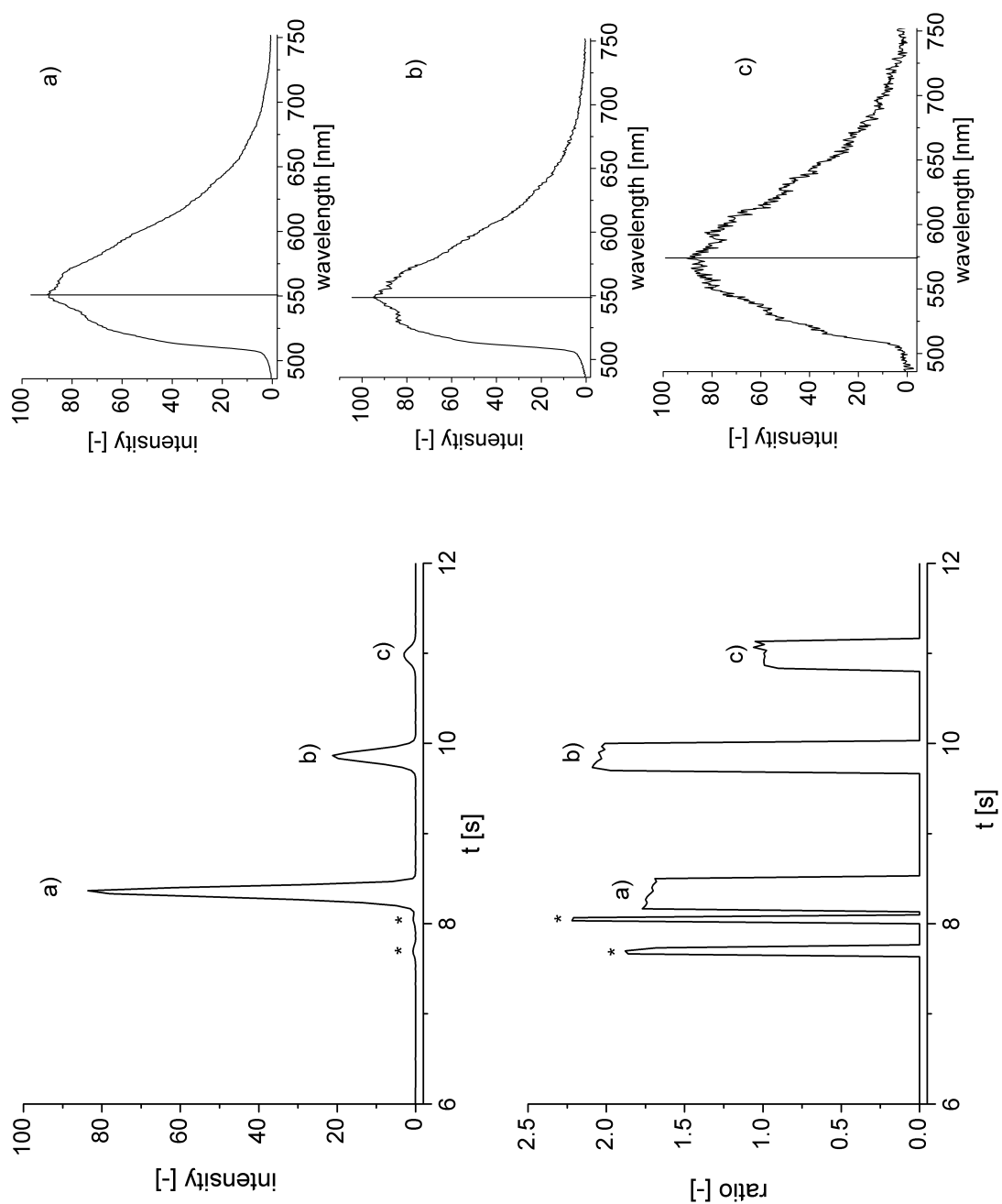
Figure 4.4: Magnification of the electropherogram of a taurine standard solution (10 mM) with corresponding peak purity plot and extracted emission spectra; a) internal standard, b) taurine derivative and c) hydrolysis product; * mark unidentified peaks.

A high emphasis was set on a very simple and fast sample preparation. Standards and real samples only had to be mixed with labeling reagent and diluted twice to ensure final taurine concentrations in the linear range of the detector system. With taurine standards covering the expected concentration range of 0.1 to 50 mmol/L (before reaction and dilution), the dynamic range of the detector was found to exceed 2.5 concentration decades, yielding a straight calibration line with an R^2 value of 0.9992. Each concentration was determined in triplicate, yielding an average standard deviation of 3.4%.

Although the derivatization procedure (including an overall 40-fold dilution of the analyte) was not optimized to obtain ultimate sensitivity, the smallest detectable amount of the taurine derivative actually injected into the separation channel was as low as 60 amol.

Eleven energy drinks and other taurine containing beverages were purchased (table 4.2) and analyzed analogous to the taurine standard solutions. Whereas most of the energy drinks exploit the legal limit of 0.4% (31.96 mmol/L) taurine content, mixed beverages based on tap water, fruit juice and also beer were found in the lower concentration range from 0.8 to 3 mmol/L. No taurine containing beverages with a medium concentration around 10-20 mmol/L could be found and used for this analysis.

Table 4.2: Taurine content determined by HPLC and on-chip CE compared with the suppliers information in mmol/L

Beverage	$c_{taurine}$ (suppl.)	$c_{taurine}$ (MCE)	$c_{taurine}$ (HPLC)
Red Bull	31.96	31.92	30.27
Red Bull sugar free	31.96	31.52	31.24
Mr. Energy	31.96	32.02	30.85
Caps energy	n/a	3.19	2.68
Effect	31.96	31.89	31.29
S1	31.96	33.49	32.19
Veltins V+ energy beer	n/a	1.85	1.45
Kick off (bottle)	31.96	33.78	32.81
Kick off (can)	2.40	3.26	2.68
Xi energy water	0.80	1.01	0.87
Xi climax	31.96	32.02	31.27

An exemplary electropherogram of a derivatized energy drink sample is shown in figure 4.5. The graph below shows the corresponding peak purity plot.

Comparable to the taurine standard solutions, the data shows no sign of co-elution. All results generated by the on-chip analysis were compared with the supplier's information and found to be in good accordance (table 4.2). The average standard deviation for all real sample measurements was 3.0 %.
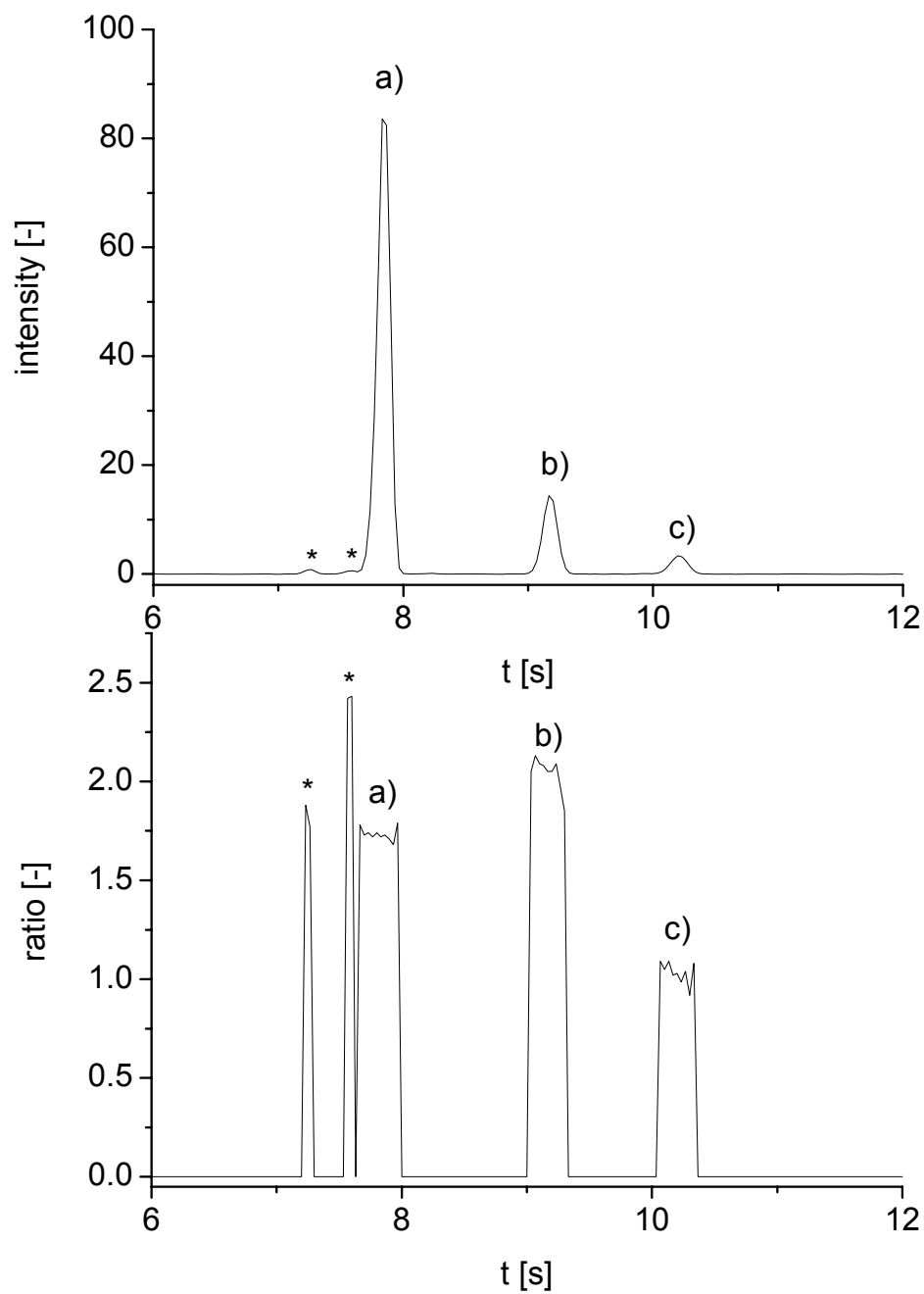
Figure 4.5: Electropherogram of a taurine real sample (Red Bull Sugar Free) with corresponding peak purity plot; a) internal standard, b) taurine derivative and c) hydrolysis product; * mark unidentified peaks
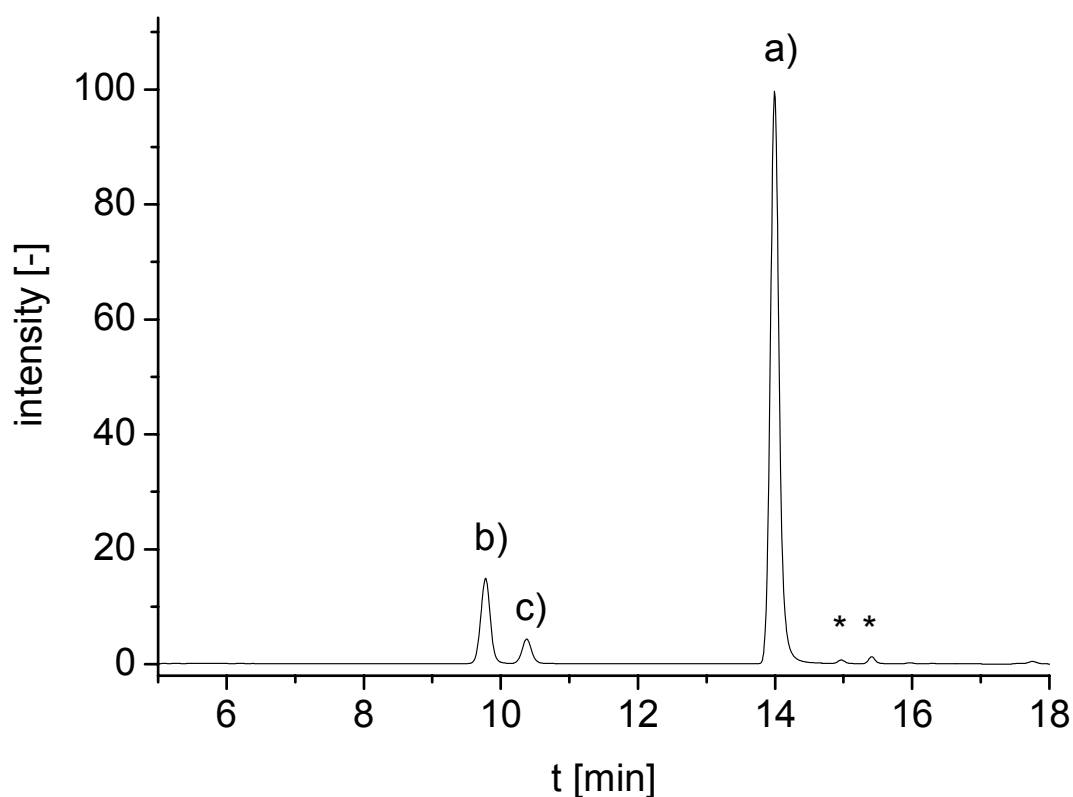
Figure 4.6: HPLC chromatogram of taurine standard solution (10 mM); a) internal standard, b) taurine derivative and c) hydrolysis product; * mark unidentified peaks

To validate the results of the microchip separation, the analysis was also performed on a commercially available HPLC system with fluorescence detection. Using a column with C18 material, the aqueous part of the acetonitrile/water gradient had to be acidified (10 mM acetate, pH 5) to ensure sufficient retention of the highly polar NBD-derivatives. Figure 4.6 shows the liquid chromatogram of a derivatized energy drink sample. In contrast to

electrophoresis, the chromatogramic separation with its different retention mechanism results in a changed elution order of the three major peaks.

The analytes are separated within 15 minutes; one complete chromatographic run takes 23 minutes. Threefold injection of the diluted reaction mixtures yielded average standard deviations of 1.8%. The resulting taurine concentrations determined by means of HPLC are in good agreement with the on-chip measurements and the supplier's information (table 4.2). Both detection methods delivered very similar results, which is obvious from the correlation plot (figure 4.7).
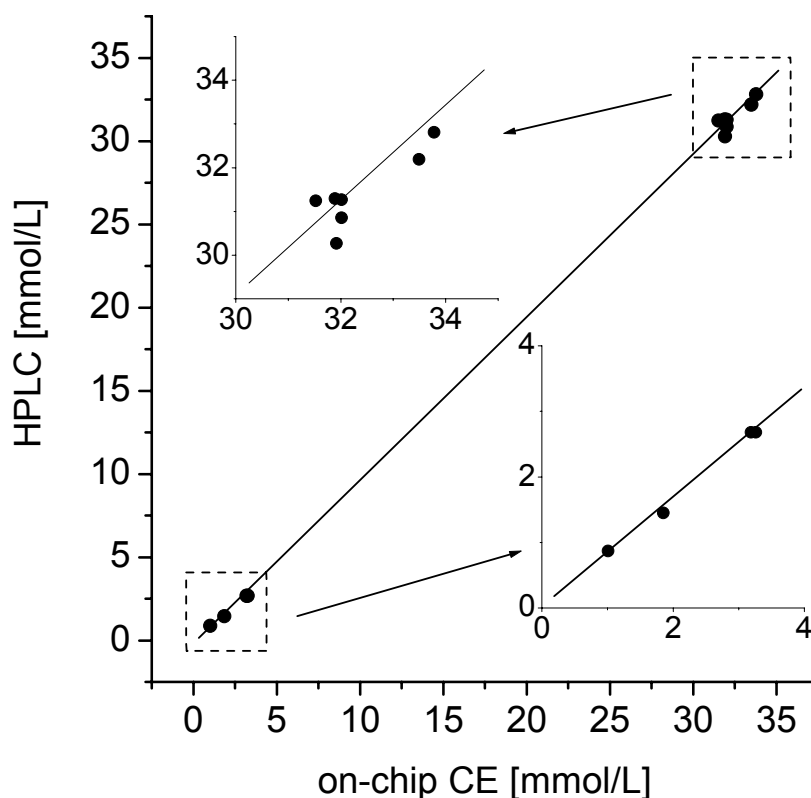

Figure 4.7: Correlation plot of HPLC and on-chip CE results of real sample measurements. Lower and higher concentration ranges have been enlarged in the inserts.

4.4 Conclusions

This work describes the development of a method for the quantitative on-chip determination of taurine in energy drinks and other taurine containing beverages. After derivatization with NBD-Cl, the sample is filled into the reservoir of a glass microchip and separated by capillary electrophoresis. Three major peaks, the internal standard, the taurine derivative and the hydrolysis product of the reagent are separated within only 12 seconds. The separation is observed with a wavelength-resolved fluorescence detector consisting of a fluorescence microscope, a spectrograph and an intensified CCD-camera. The yielded information-rich electropherogram shows even subtle differences in the fluorescent properties of the observed analytes. Furthermore, it enables peak purity calculations, ensuring no hidden coelution is taking place. Including only dilution and addition of the labeling reagent, a very fast and straightforward sample preparation method was applied, which was adapted to the anticipated taurine concentrations in real samples. A calibration curve with standards covering the expected concentration range from 0.1 to 50 mmol/L was recorded. The smallest detectable amount (S/N = 3) of taurine derivative actually injected into the separation channel was 60 amol. The method was successfully validated by liquid chromatography with fluorescence detection.

4.5 References

1.   Terry S C (1997) IEEE Trans Electron Devices 26:1880-1886

2.   Manz A, Graber N, Widmer H M (1990) Sens Actuators, B 1:244-248

3.   Harrison D J, Manz A, Fan Z, Lüdi H, Widmer H M (1992) Anal Chem 64:1926-1932

4.   Ros A, Hellmich W, Duong T, Anselmetti D (2004) J Biotechnol 112:65-72

5.   Jacobsen S C, Koutny L B, Hergenröder R, Moore A W, Ramsey J M (1994) Anal Chem 66:3472-3476

6.   Hellmich W, Pelargus C, Leffhalm K, Ros A, Anselmetti D (2005) Electrophoresis 26:3689-3696

7.   Piehl N, Ludwig M, Belder D (2004) Electrophoresis 25:3848-3852

8.   Greenway G M, Haswell S J, Petsul P H (1999) Anal Chim Acta 387:1-10

9.   Malcik N, Ferrance J P, Landers J P, Caglar P (2005) Sens Actuators, B 107:24-31

10.   Vrouwe E X, Luttge R, Olthuis W, van den Berg A (2005) Electrophoresis 26:3032-3042

11.   Garcia C D, Engling G, Herckes P, Collett J L, Henry C S (2005) Environ Sci Technol 39:618-623

12.   Wang J, Zima J, Lawrence N S, Chatrathi M P, Mulchandani A, Collins G E (2004) Anal Chem 76:4721-4726

13.   Pasas S A, Lacher N A, Davies M I, Lunte S M (2002) Electrophoresis 23:759-766

14.   Macka M, Andersson P, Haddad P R (1998) Anal Chem 70:743-749

15.   Oki A, Takamura Y, Ito Y, Horiike Y (2002) Electrophoresis 23:2860-2864

16.   Rodriguez I, Chandrasekhar N (2005) Electrophoresis 26:1114-1121

17.   Belder D, Ludwig M (2003) Electrophoresis 24:3595-3606

18.   Petersen N J, Nikolajsen R P H, Mogensen K B, Kutter J P (2004) Electrophoresis 25:253-269

19.   Milei J, Ferreira R, Llesuy S, Forcada P, Covarrubias J, Boveris A (1992) Am Heart J 123:339-345

20.   Huxtable R J, Sebring L A (1986) Trends Pharmacol Sci 7:481-485

21.   Rhuxtable R J (1992) Physiol Rev 72:101-163

22.   Hartley S G, Goodman H O, Shihabi Z (1989) Neurochem Res 14:149-152

23.   Bhatnagar S K, Welty J D, Al Yussuf A R (1990) Int J Cardiol 27:361-366

24.   Gray G E, Landel A M, Meguid M M (1990) Nutrition 10:11-15

25.   Schuller-Levis G B, Park E (2003) FEMS Microbiol Lett 226:195-202

26.   Cataldi T R I, Telesca G, Bianco G, Nardiello D (2004) Talanta 64:626-630

27.   Muo S, Ding X, Liu Y (2002) J Chromatogr, B 781:251-267

28.   Waterfield C J (1994) J Chromatogr, B 657:37-45

29.   Chen Z, Xu G, Specht K, Yang R, She S (1994) Anal Chim Acta 296:249-253

30.   Sakai T, Nagasawa T (1992) J Chromatogr 576:155-157

31. McMahon G P, O'Kennedy R, Kelly M T (1996) J Pharm Biomed Anal 14:1287-1294

32. Qu F, Qi Z, Liu K, Mou S (1999) J Chromatogr, B 730:161-166

33. Kelly M T, Fabre H, Perett D (2000) Electrophoresis 21:699-705

34. Götz S, Karst U (2006), submitted for publication

Chapter 5

Quantitative Analysis of Thiols in Consumer Products on a Microfluidic Capillary Electrophoresis Chip with Fluorescence Detection[‡]

A microchip capillary electrophoresis-based method for the quantification of the thiols mercaptoacetic acid (MAA) and 2-mercaptopropionic acid (2-MPA) in depilatory cream and cold wave suspensions was developed. The thiols were first derivatized with the fluorogenic reagent ammonium-7-fluorobenzo-2-oxa-1,3-diazole-4-sulfonate (SBD-F). The derivatives were separated within only 20 seconds by microchip capillary electrophoresis (MCE) and detected by their fluorescence. Conventional capillary electrophoresis with diode-array detection and liquid chromatography with fluorescence detection were used for validation. An internal standard provided relative standard deviations for multiple injections of only 4% or less for the MCE approach. Limit of detection is 2 µM, limit of quantification 6 µM and the linear range comprises nearly three decades of concentration starting at the limit of quantification.

5.1 Introduction

In the last few years, intense research activities were directed towards the miniaturization of analytical methods, with a particular focus on the design and use of microchips [1,2]. Although many attractive approaches have been published, most of them were presented as proof of principle only. Few papers, however, focus on the truly quantitative analysis on microchips. Capillary electrophoresis is one of the driving forces used in microchip technology due to its separation efficiency for polar analytes.

The determination of inorganic ions, e.g. lithium in blood [3,4], anions and cations in tap water [5], nitrite in water [6] and calcium in urine [7], has been described. While most of this work relies on capillary zone electrophoresis (CZE), isotachophoretic approaches have been presented as well [8,9]. Further examples for quantitative MCE include organic molecules like oxalate in urine [10], carnitines in water [11], 4-amino-3-methyl-N-ethyl-N-(β-methane sulfonamidoethyl)aniline in photographic developer [12], levoglucosan in aerosols [13], thiols in nerve agent degradation products [14] and homocysteine in plasma [15]. Semi-quantitative approaches are known for biological and medical applications like DNA in restriction digests of adenovirus 2 [16] and hepatitis C viruses in clinical patients [17].

Different detection principles can be combined with CE or MCE such as optical methods, electrochemical detection or even mass spectrometry [18-21].

Optical techniques are well established and have the advantage of freely selecting the detection volume on an existing glass microchip. Fluorescence detection is inherently more sensitive than UV detection and frequently, derivatization reactions have to be carried out.

The derivatization of thiols has two major reasons: One is to stabilize the reactive thiol functionality, because thiols are known to form sulfide bridges and can easily be oxidized [22]. The second is an increase in the sensitivity of detection. Many different labeling agents for the derivatization of thiols are known [22,23]. 7-Fluorobenzo-2-oxa-1,3-diazole-4-sulfonate (SBD-F) has incorporated a negative charge in the sulfonyl functionality, it is highly water-soluble and easily amenable to electrophoresis. Furthermore, it is highly reactive towards thiol groups and, in contrast to the reaction products, the reagent itself is not fluorescent [24]. It is also known for its stability, as it is stable in borate buffer (pH 9.5) at room temperature for at least one week [25]. Dissolved SBD-thiol derivatives can be stored for more than a week in the refrigerator. Fluorescence is measured with excitation at 380 nm and emission at 515 nm for most SBD thiol derivatives [24].

Commercial depilatory cream and cold wave suspensions contain mercaptoethanoic acid (MAA) (also known as mercaptoacetic acid or thioglycolic acid), 2-mercaptopropionic acid (2-MPA) (thiolactic acid), 3-mercaptopropionic acid (3-MPA) or a mixture of these [26]. According to German legislation, depilatory cream for private use may contain up to 5%, and cold wave lotions may contain up to 8% of this acid (11 % for professional use) [27]. These concentrations are calculated as of the free acid. The

standard procedure for the determination of the thiol content proposed by EU legislation is a iodometric titration. As titrations do always yield a sum parameter, a GC analysis after derivatization is suggested for samples containing more than one thiol. This GC analysis employs overnight derivatization with diazomethane as derivatization agent after precipitation of thiols with cadmium acetate [28].

In this chapter, the development of a new method for the determination of thiols in cosmetics after their derivatization with SBD-F is described. A CE-DAD method is developed and transferred to MCE/fluorescence and compared to the results of HPLC/fluorescence measurements. Microchip analysis requires only small amounts of sample and reagent, and separation times can be reduced compared to conventional methods.

5.2 Experimental

5.2.1 Materials, Chemicals and Samples

Boric acid, EDTA, sodium hydroxide and citric acid were purchased from Merck (Darmstadt, Germany). Mercaptoacetic acid (MAA), 2-mercaptopropionic acid (2-MPA) and 3-mercaptopropionic acid (3-MPA) were obtained from Aldrich (Steinheim, Germany). Hydrochloric acid was purchased from Acros (Geel, Belgium) and water was purified by a Millipore-Q plus water cleaning system from Millipore (Billerica, MA, USA). SBD-F was synthesized according to literature [24,29].

Ten cold wave lotion and depilatory cream samples from different manufacturers were purchased from retail stores in Germany, The Netherlands and the United States. Two samples were cold wave suspensions; eight were different preparation of depilatory agents like cream, mousse or foam.

5.2.2 Buffer and Standard Preparation

The 50 mM borate buffer pH 9.50 containing 5 mM of EDTA was prepared by weighing in solid substances. After adding 800 mL of Milli-Q water, it was titrated with 1 M or 100 mM sodium hydroxide solution to a pH of 9.5 prior to filling up to 1 L. Citrate running buffers were prepared in the same way, and stored at 4°C. All buffers were filtered through a 0.45 μm nylon syringe filter (Alltech, Breda, The Netherlands) after preparation.

Thiol standards were prepared by dissolving the thiols in borate buffer. For all further dilutions and mixings, borate buffer was used as a solvent.

5.2.3 Derivatization Procedure and Sample Preparation

Between one and two milligrams of cream sample were dissolved in 0.5 mL of borate buffer. Then, the internal standard solution and 470 µl, minus the volume of the internal standard solution, of a 10 mM SBD-F solution in reaction buffer were added. The closed vial was heated in a water bath at 60°C for one hour. After cooling down to room temperature, 30 µL of 2 M hydrochloric acid were added to acidify the solution. All further reaction parameters were adjusted as described in literature [30].

For cold wave suspensions and thiol standards, the same basic derivatization procedure was followed, but for these, the diluted sample (with borate buffer) or calibration standards prepared in borate buffer were used. All measurements were performed within one week after derivatization and storage of the solutions at 4°C, which is, according to reference [30], a reasonable timescale for storage of dissolved SBD-derivatives.

5.2.4 CE, MCE and HPLC Separation Conditions

CE experiments were performed on an Agilent [3D]HPCE instrument equipped with a diode-array detector (Agilent, Waldbronn, Germany). Fused silica capillaries were obtained from Polymicro Technologies (Phoenix, AZ, USA). CE separations were performed on a 32 cm capillary with an effective length of 23.5 cm and an inner diameter of 75 µm. Prior to each series of experiments, capillaries were conditioned for 25 min with 1 M NaOH solution and were then flushed with water and citrate running buffer (one minute each). The running buffer had a pH of 4.4 and a concentration of 20 mmol/L. Between the measurements, the capillary was flushed for half a minute with buffer from a separate vial into a waste vial. Samples were introduced hydrodynamically by applying a pressure of 50 hPa for 1 s. A separation voltage of -28 kV was applied for 1.3 min. To detect SBD-thiol derivatives, an absorption wavelength of 383 nm was selected and 320 nm were used for detecting the SBD-F reagent.

T3550 glass microchips for capillary electrophoresis were purchased from Micronit Microfluidics (Enschede, The Netherlands) with a channel width of 50 µm and depth of 20 µm. A channel of 5 mm length transports buffer or sample solutions to the injection cross. The separation pathlength is 35 mm with 26 mm from the double tee injector to the position of the detection volume. An ECH-135L high voltage power supply (Micronit Microfluidics) with a custom made outlet for a TTL trigger signal was combined with an in-house built chip holder including platinum electrodes made from Pt wire (0.25 mm

diameter). Microchip separations were performed with a 100 mM citrate buffer pH 4.4. Voltages applied during injection and separation are shown in table 5.1.

Table 5.1: Voltages applied to the microchip reservoirs.

reservoir	injection (10 s) [V]	separation (30 s) [V]
sample	1500	1000
sample waste	3000	1000
buffer	1800	0
buffer waste	0	3000

The chip was flushed with buffer and all reservoirs were refilled with 2.5 µL solution prior to each measurement. Flushing of microchip channels was performed with a 500 µL syringe (SGE, Ringwood, Australia) equipped with a Teflon liner (Upchurch Scientific, Oak Harbor, WA, USA).

HPLC measurements were performed using a Shimadzu (Duisburg, Germany) HPLC system consisting of two LC-10AS pumps, GT-154 degasser unit, SIL-10A autosampler, SPD-M10Avp diode-array detector, RF-10AXL fluorescence detector, and CBM-10A controller unit with class LC-10 software version 1.6. A 4.6 x 150 mm Eclipse C8 RP column (Agilent, Waldbronn, Germany) with 5 µm particles was used for LC separations. The mobile phase

consisted of acetonitrile and 20 mM phosphate buffer at pH 3.0 and was used for gradient elution. In the first four minutes, the ACN content was increased from 10 to 20 %. In the following three minutes, it was gradually increased up to 40%.

5.2.5 Fluorescence Microscope and Data Analysis

The fluorescence microscope-based set-up consists of an inverse IX-71 fluorescence microscope (Olympus, Hamburg, Germany), an Olympus xenon lamp (U-LH75XEAPO), a SpectraPro 308i spectrograph (Acton Research, Acton, MA, USA) equipped with a 150 grooves per mm (gr/mm) grating and a light intensified CCD-camera PI-Max 512RB from Princeton Instruments (Trenton, NJ, USA) that was combined with a ST133 controller ver.5 (Princeton Instruments).

Data recording and evaluation was performed by WinSpec/32 software version 2.5.12.0 (Princeton Instruments). For wavelength selection, a filter cube with components from Chroma (Rockingham, VT, USA) was employed (exciter: D390/70X; dichroic: 440DCXR; emitter: HQ500LP).

This set-up can be used in combination with the commercial CE instrument or for detection of microchip separations. For a detailed description of this detector see Chapter 3. After exporting the raw data, all electropherograms were integrated using 3D-CE ChemStation software revision A 08.03 (Agilent, Waldbronn, Germany).

Fluorescence spectra were recorded with an Aminco Bowman series 2 fluorescence spectrophotometer (now Thermo Electron, Dreieich, Germany) with AB 2 software version 5.00. Measurements with organic solvents contain 10% of aqueous borate buffer at pH 9.5.

5.3 Results and discussion

5.3.1 Fluorescence Properties of SBD-Thiol Derivatives

In order to determine the properties of the SBD-thiol derivatives for CE separation and detection, the effects of buffer composition and pH on fluorescence intensities and emission wavelength were tested. In figure 5.1, fluorescence spectra of four different thiol-SBD derivatives are presented.
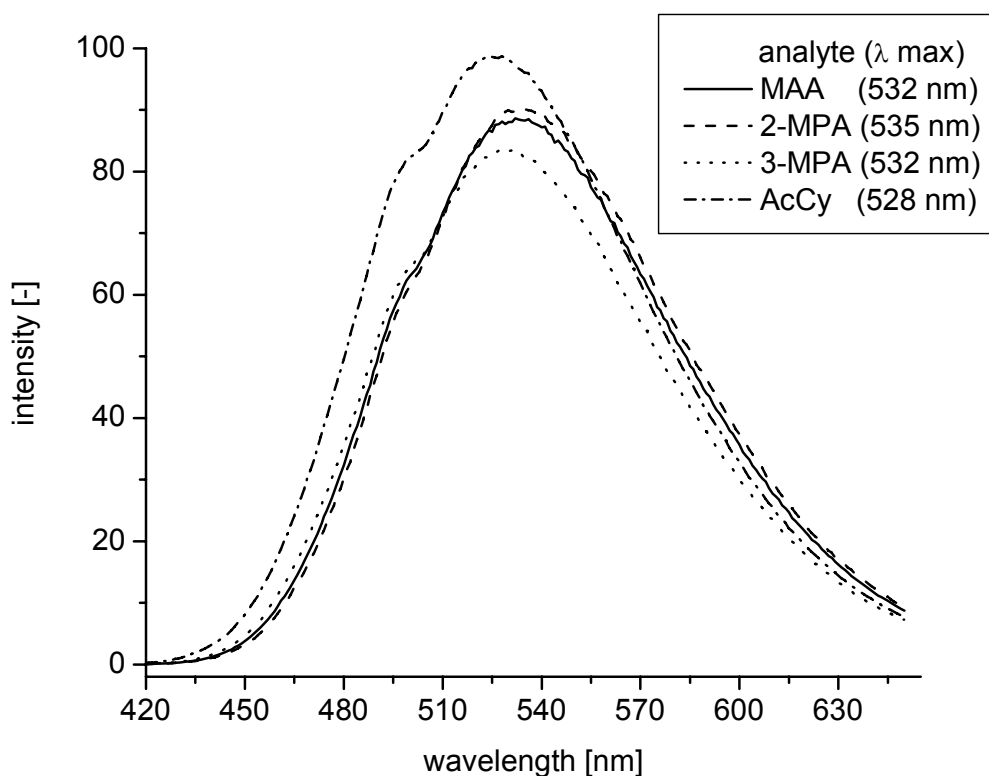

Figure 5.1: Emission spectra of four different SBD-thiol derivatives recorded with an excitation wavelength of 380 nm in aqueous borate buffer (pH 9.5) containing 5 mM EDTA.

Excited at 380 nm, the wavelength of the intensity maxima varies slightly depending on the individual thiol. The emission maximum of the acetyl cysteine derivative (528 nm), for example, is 7 nm lower than that of 2-MPA (535 nm) under the given conditions.

In contrast to the SBD-cysteine derivative [30], the mercaptoacetic acid derivative does not show a significant pH dependence of its fluorescence intensity. However, fluorescence intensities can well be altered by addition of organic solvents (figure 5.2).
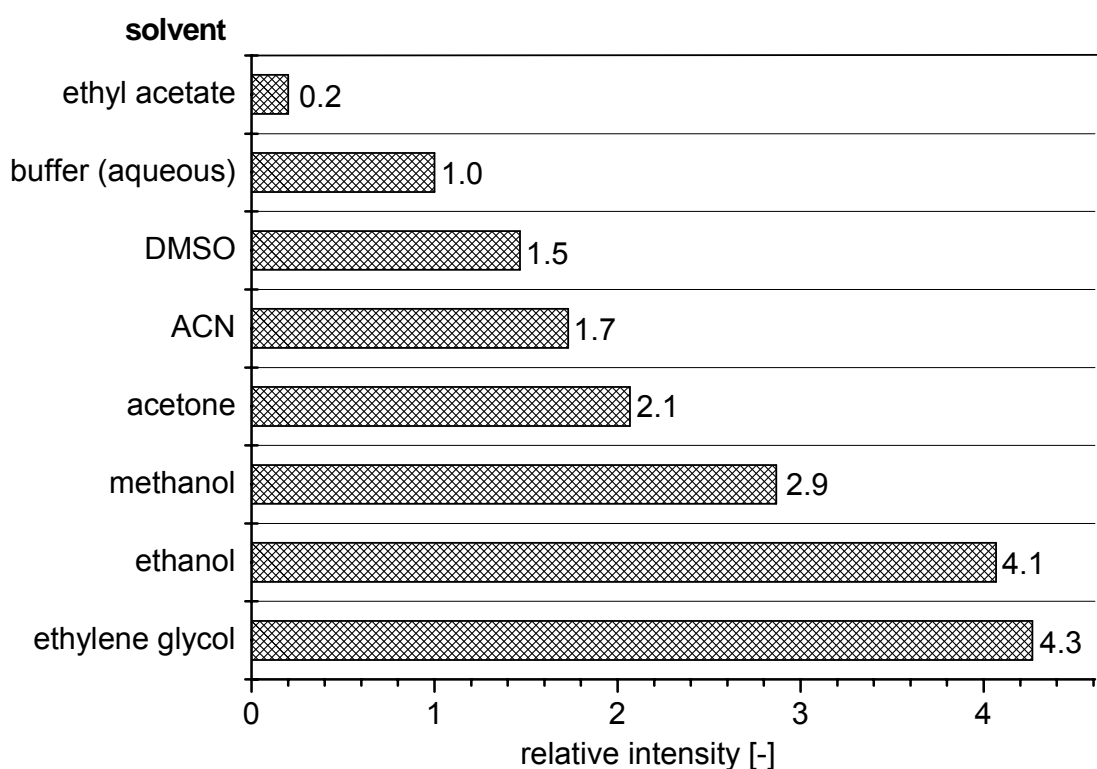
solvent

Figure 5.2: Relative fluorescence intensities of the MAA-SBD derivative in different organic solvents (containing 10% aqueous reaction solution).

The highest intensities were obtained upon the addition of ethanol or ethylene glycol with an increase by a factor of approximately four compared with an aqueous solution at pH 9.5, which is sodium borate buffered. Slightly higher intensities than with this borate buffer were obtained after addition of methanol, acetone, DMSO and ACN. Lower intensities were obtained from the addition of ethyl acetate. Dissolving the derivatives in organic solvents also results in a shift of emission maxima to lower wavelengths. The addition of a solvent with an alcohol moiety (ethanol, methanol and ethylene glycol) lowers the wavelength by approximately 15 nm; for all other tested organic solvents, a shift of approximately 35 nm was observed.

5.3.2 Optimization of Electrophoretic Separations

The non-derivatized thiols as well as the internal standard are weak acids. After derivatization, the acid functionality remains unaltered and the SBD-F reagent adds a sulfonyl functionality. Therefore, all molecules are negatively charged, which renders the derivatives to be quickly moving in the negative CE mode.

Different pH values and compositions were tested in this work. Fine-tuning of the pH value in the range of pH 3.79 to pH 4.50 of a sodium citrate buffer is shown in figure 5.3. By changing the pH value of the running buffer from 3.79 to 4.27, the elution order is changed and the SBD-F peak is shifted to the end of the separation. The separation is completed after 48 s using a pH of 4.50 compared to 70 s (pH 3.79). Peak shape is also changing during this series.

Running buffer of pH 4.36 yielded the most symmetric peaks. A 20 mM sodium citrate buffer with a pH value of 4.36 was finally selected due to the parameters elution order, separation time and peak shape. Generally, it is advantageous to have the reagent peak eluting last, as there are no interferences with analyte peaks to be expected and as the measurement may be stopped earlier. This requirement is well achieved in the described separation system.
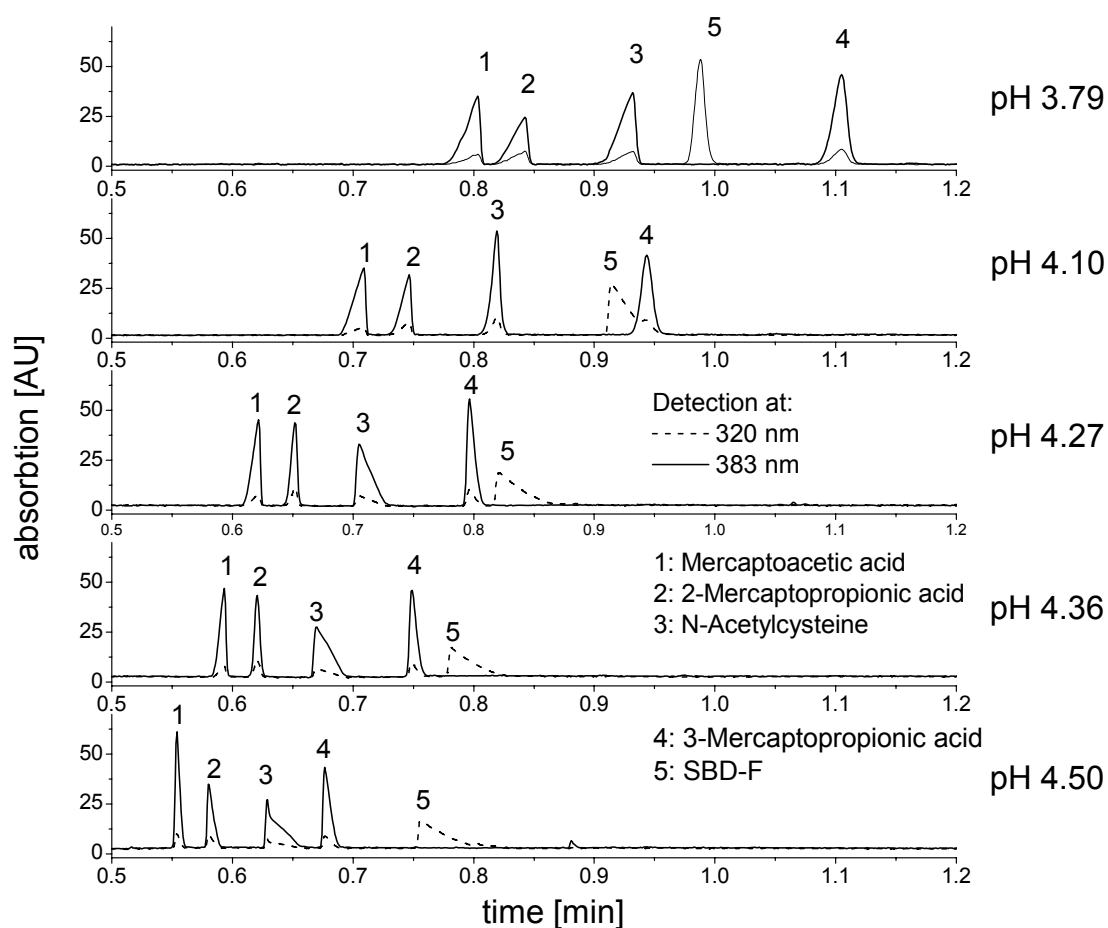

Figure 5.3: Optimization of the pH value of the separation buffer. A mixture of four different SBD-thiol derivatives was used to test the conditions. Electropherograms were recorded on a CE/DAD system.

5.3.3 Microchip Separations

Figure 5.4 depicts an electropherogram of the separation of a solution containing three different SBD-thiol derivatives (MAA, 2-MPA, 3-MPA). This separation was obtained after transferring the method from the CE/DAD system to the microchip. As fluorescence is used for detection on the microchip, the SBD-F reagent is not detected, but it is expected to elute after the last peak, as the peak order is the same compared to conventional CE. A 100 mM concentration of the running buffer was selected for this technique, as injections worked better due to the similarity of electrolyte concentration in sample solutions and running buffer.
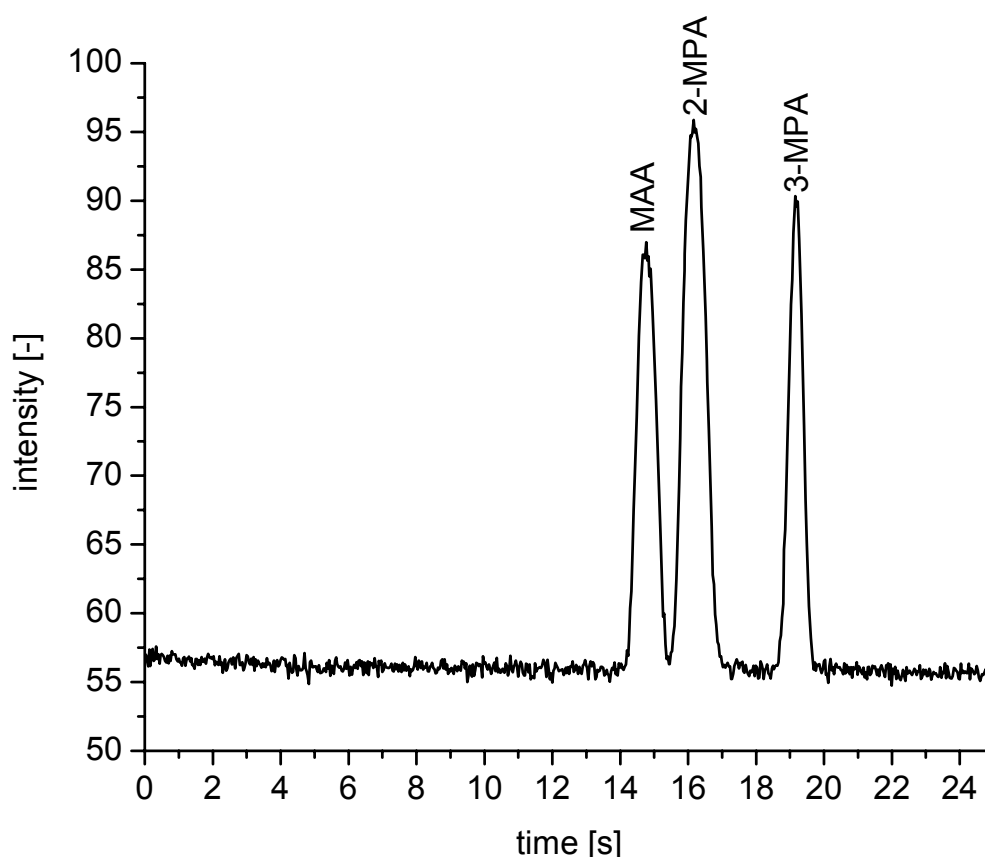

Figure 5.4: Electropherogram of a mixture of three different thiols (MAA, 2-MPA and 3-MPA) obtained from a microchip separation with fluorescence detection.

For the determination with MCE, an internal standard is essential to compensate for experimental errors. The biggest source of error is related to the coupling of the microchip with the detector. Although the microchip is fixed by the chip holder, there is still some variability, so that the separation channel is not necessarily projected into the entrance slit of the spectrograph. Using a 40 fold magnification objective instead of 20 fold magnification reduces the experimental error to less than 10% RSD. After employing an internal standard, the variations of the peak area were reduced to a level comparable with conventional CE measurements (less than 4 % RSD). This procedure also compensates for various other experimental errors made during measurement (injection volume, migration speed) or variations in sample preparation.

5.3.4 Comparison of HPLC, CE and MCE Measurements

On-chip measurements were compared with results obtained from CE/DAD and HPLC/fluorescence instruments. All three instruments were therefore tested with the same set of solutions. All stated concentrations are concentrations of thiol before derivatization and dilutions were also made before derivatizing the solutions.

Limits of detection for MAA were 20 µM for the CE/DAD system. A LOD of 2 µM was determined for on-chip measurements with fluorescence detection. The value for HPLC/fluorescence is also 20 µM, although the solutions were diluted by a factor of 100, as the undiluted highest concentrated solution

provides a signal exceeding the upper limit of the fluorescence detector. This means that the detection limit of the instrument is theoretically one decade lower than achieved by chip CE.

The linear range for the determination of thiols ranges from 50 µM to 2 mM for CE/DAD and HPLC/fluorescence and 5 µM to 2 mM for MCE/fluorescence measurements. At the lower end, the range is restricted by the quantification limit of the analytical instrumentation and the upper end is limited by the reagent excess. A detailed description of the comparison of analytical results for the quantification is presented in the following paragraph.

5.3.5 Quantification of Thiols in Depilatory Cream and Cold Wave Suspensions

Thiol concentrations in ten different cosmetic samples were determined by three different instruments: CE/DAD, HPLC/fluorescence and MCE/fluorescence. Table 5.2 shows the mass percentage of thiol in different depilatory creams and cold waving suspensions. After applying all described corrections, RSD values are below 4% (N=3) and the determined values of all three instruments are within the error margins. Application of the internal standard does not only decrease the RSD values of the microchip measurements, but it is also the base for the successful validation of the data by HPLC and conventional CE.

Table 5.2: Determined MAA contents of 9 depilatory creams and 2 cold wave suspensions in mass percent; results for all three detection systems are shown with their corresponding standard deviations (N=3).

	MCE	RSD [%]	HPLC	RSD [%]	CE	RSD [%]
Isana	2.37	2.91	2.48	1.82	2.10	2.80
Nair	3.30	0.27	3.30	1.49	2.88	2.01
Sally Hansen	2.96	0.80	3.02	0.81	2.70	1.63
Veet "rosa"	4.44	0.61	4.48	0.77	3.84	2.20
Veet "blau"	3.22	1.73	3.30	0.95	2.75	4.00
Pilca (creme)	2.77	2.06	2.96	0.81	2.41	2.74
Pilca (mousse)	4.00	1.22	4.36	1.68	3.47	1.85
Snä	6.11	3.88	6.42	1.70	5.01	1.81
cold wave (mild)	7.00	3.43	7.72	0.05	5.69	3.47
cold wave (strong)	6.85	2.51	7.47	0.92	5.57	0.63

5.3.6 Discussion

A new analytical method for the quantification of thiols in depilatory cream and cold wave suspensions is presented. The developed separation conditions for the commercial CE system were transferred to the MCE format. On the chip,

a baseline separation including an internal standard was achieved within 20 seconds. It was demonstrated that the results obtained by microchip capillary electrophoresis are compatible with those achieved by classical methods like HPLC and CE separations. Quantitative results of all three tested instruments are in good agreement, and RSD values are below 4% for MCE separations after correction by an internal standard. For analysis, only small amounts of sample and reagents were necessary, and glass microchips could easily be reused after cleaning.

Future work will deal with the integration of the derivatization onto the chip and the automation of microchip rinsing and filling procedures in order to further improve robustness and reproducibility of the microchip technology.

5.4 References

1.   Reyes D R, Iossifidis D, Auroux P A, Manz A (2002) Anal Chem 74:2623-2636

2.   Auroux P A, Iossifidis D, Reyes D R, Manz A (2002) Anal Chem 74:2637-2652

3.   Vrouwe E X, Luttge R, van den Berg A (2004) Electrophoresis 25:1660-1667

4.   Vrouwe E X, Luttge R, Olthuis W, van den Berg A (2005) Electrophoresis 26:3032-3042

5.   Vrouwe E X, Luttge R, Olthuis W, van den Berg A (2006) J Chromatogr, A 1102:287-293

6.   Greenway G M, Haswell S J, Petsul P H (1999) Anal Chim Acta 387:1-10

7.   Malcik N, Ferrance J P, Landers J P, Caglar P (2005) Sens Actuators, B 107:24-31

8.   Masar M, Zuborova M, Bielcikova J, Kaniansky D, Johnck M, Stanislawski B (2001) J Chromatogr, A 916:101-111

9.   Bodor R, Madajova V, Kaniansky D, Masar M, Johnck M, Stanislawski B (2001) J Chromatogr, A 916:155-165

10.   Zuborova M, Masar M, Kaniansky D, Johnck M, Stanislawski B (2002) Electrophoresis 23:774-781

11.   Kameoka J, Craighead H G, Zhang H W, Henion J (2001) Anal Chem 73:1935-1941

12.   Sirichai S, de Mello A J (1999) Analyst 125:133-137

13.   Garcia C D, Engling G, Herckes P, Collett J L, Henry C S (2005)
       Environ Sci Technol 39:618-623

14.   Wang J, Zima J, Lawrence N S, Chatrathi M P, Mulchandani A, Collins
       G E (2004) Anal Chem 76:4721-4726

15.   Pasas S A, Lacher N A, Davies M I, Lunte S M (2002) Electrophoresis
       23:759-766

16.   Mueller O, Hahnenberger K, Dittmann M, Yee H, Dubrow R, Nagle R,
       Ilsley D (2000) Electrophoresis 21:128-134

17.   Young K C, Lien H M, Lin C C, Chang T T, Lee G B, Chen S H (2002)
       Talanta 56:323-330

18.   Uchiyama K, Nakajima H, Hobo T (2004) Anal Bioanal Chem 379:375-
       382

19.   Schwarz M A, Hauser P C (2001) Lab Chip 1:1-6

20.   Mogensen K B, Klank H, Kutter J P (2004) Electrophoresis 25:3498-
       3512

21.   Vandaveer W R, Pasas-Farmer S A, Fischer D J, Frankenfeld C N,
       Lunte S M (2004) Electrophoresis 25:3528-3549

22.   Shimada K, Mitamura K (1994) J Chromatogr, B 659:227-241

23.   Waterval J C M, Lingeman H, Bult A, Underberg W J M (2000)
       Electrophoresis 21:4029-4045

24.   Imai K, Toyo'oka T, Watanabe Y (1983) Anal Biochem 128:471-473

25.   Imai K, Uzu S, Toyooka T (1989) J Pharm Biomed Anal 7:1395-1403

26.   Falbe J, Regitz M (1999) Römpp Lexikon Chemie, Georg Thieme
       Verlag, Stuttgart, pp. 2594, 4523, 4525-4526

27.   Horst M, Mrohs A (2005) Lebensmittelrecht auf CD-Rom, Behr's Verlag

       GmbH & Co. KG, Hamburg 2005, Kosmetik-Verordnung vom 7.

       Oktober 1997

28.   European Commision, Enterprise Directorate-General,

       Pharmaceuticals and cosmetics: Cosmetics legislation, Cosmetic

       Products, Vol. 2: Methods of analysis, Office for Official Publications of

       the European Communities, Luxembourg, 2000, pp. 80-88

29.   Di Nunno L, Florio S, Todesco P E (1970) J Chem Soc (C) 1433-1434

30.   Toyo'oka T, Imai K (1984) Analyst 109:1003-1007

Chapter 6

Concluding Remarks and Future Perspectives

In contrast to the predominantly used laser-induced fluorescence (LIF) detection methods, wavelength-resolved fluorescence detection with lamp-based excitation is a much more flexible approach that delivers additional information about the observed analytes. Despite the unrivalled sensitivity of LIF detection systems, the spectral evaluation of the emitted light can be advantageous, if more complex samples are analyzed.

The fast MCE separation of three rhodamine dyes described in chapter 3 shows how the additional information of the recorded online emission spectra can be utilized. In contrast to single wavelength detection systems, the analytes can directly be assigned to their corresponding peaks by comparison of their fluorescence emission maxima. By calculating the signal intensity ratio of two selected wavelengths, apparent in all observed spectra, a peak purity plot can be generated. Applying this method of evaluation, the hidden co-elution of an impurity in one of the commercial dyes can easily be detected.

To prove the applicability of the developed detector set-up for real samples, it is used to analyze the taurine content in beverages (chapter 4). The

developed method is the fastest separation of NBD-labeled taurine known so far (12 seconds). While a very good linearity over a dynamic range of almost three decades could be obtained, the measurements were validated by liquid chromatography. Analysis times of approximately 15 minutes for the HPLC separation clearly demonstrate the advantages of microchip capillary electrophoresis.

Furthermore, the detector was used for the determination of the active ingredients in depilatory cream and cold wave suspensions (chapter 5). The separation of the fluorescently-labeled thiol compounds could be achieved within 20 seconds. The use of different excitation and emission wavelengths for these derivatives compared with the taurine determination further demonstrates the flexibility of the developed detector system.

The results presented in this thesis clearly demonstrate the usefulness and applicability of the newly developed wavelength-resolved detection system for microchip capillary electrophoresis. Considering the complexity of many chemical and biological samples, the additional spectral information yielded with this set-up will, in many cases, be more valuable than the ultra-low limits of detection of rather inflexible LIF detection systems.

Although very fast microchip separations have been presented, the sample throughput of those measurements is still rather low due to the required manual cleaning steps between the measurements. The development of an autosampler system, which can perform operations including etching, flushing

and cleaning of the chip as well as the application of sample and buffer solution, could be a big step towards a high-throughput analysis system.

To fully exploit the potential and to further improve the sensitivity of the detector set-up, time-resolved fluorescence measurements shall be conducted in future work. In combination with a pulsed excitation source (e.g. a high frequency, high output LED), the fast gating ability of the intensified CCD-camera (2 ns gate width) enables time-delayed detection of the fluorescent signal. This method shall allow significant reduction of background signal originating from excitation light and fast-decaying Raman scattering. By manipulating the gate-delay and shifting the detection time frame, fluorescence decay curves shall be recorded. Evaluating fluorescence lifetimes shall add another dimension of information to the detection method.

The fact that the CCD-chip is a two-dimensional detector enables spatial observations, while the wavelength information is still being preserved. This feature could, in future work, be used for the wavelength-resolved detection of multiple separations on a single microchip, simultaneously performed in parallel channels.

Summary

This thesis describes the development and application of a new wavelength-resolved CCD-based fluorescence detector for microchip separations.

In recent years, miniaturization has been one of the major trends in the development of new analytical separation systems. As the manipulated sample amounts and detection volumes on microchips have become smaller and smaller, the need for high-performance detection systems has never been more relevant. Applied methods of detection have to be well adapted to the small dimensions and high speed of microchip separations.

Chapter 2 reviews recent developments in optical detection methods for microchip separations and highlights interesting new approaches for high-performance detection techniques. UV/vis spectroscopy, as one of the established methods for detection in liquid phase separation systems, plays only a minor role in microchip CE, because the very short optical pathlengths available on microchips allow only for rather low sensitivity. Fluorescence detection, however, can easily be adapted to microchip format, if highly focused excitation light is used. Excellent results are achieved with laser-induced fluorescence (LIF), because the highly coherent laser beam is easily focused onto tiny detection volumes, thus yielding a very high irradiation. The combination with a highly sensitive detector, such as a photomultiplier tube (PMT), yields the lowest limits of detection that are possible at the moment.

However, little or no chemical and structural information is provided about the analyte.

To increase the degree of information from a microchip capillary electrophoresis (MCE) separation, this work focuses on the attractive approach to add spectral information to fluorescence detection by dispersing the emitted light, thus enabling the recording of complete on-line emission spectra. Consisting of a fluorescence microscope with a tunable lamp-based excitation source, a spectrograph and an intensified CCD-camera, this set-up forms a flexible and powerful detector system, well adapted to MCE separations. The detection of the dispersed emission light delivers wavelength-resolved electropherograms. Comparable to a diode-array detector in UV/vis absorbance, the detection of complete emission spectra during the separation yields valuable additional information about the analytes.

Chapter 3 deals with the development of the detector set-up and describes the implemented components in detail. Serving as a model system, the electrophoretic separation of three rhodamine dyes with different fluorescent properties shows the performance of the instrument. Submicromolar concentrations are detected, and the additional dimension of information gained by the wavelength-resolved detection is used for peak assignment and peak purity measurements. Utilizing such a method of evaluation, hidden co-elution can readily be spotted.

As quantitative and reproducible analyses on microchips are still challenging, the applicability of the newly developed detector system to real samples is described in chapter 4. This part of the thesis focuses on the quantitative determination of the taurine content in beverages. More than ten energy and sports drinks and other taurine-containing beverages were analyzed by MCE. The fastest separation of fluorescently-labeled taurine derivatives known so far (12 seconds) could be achieved. Showing good linearity over a wide concentration range, the wavelength-resolved detection system was successfully applied and validated by an independent HPLC method.

Chapter 5 deals with the determination of thiol compounds in consumer products. The active ingredients of depilatory cream and cold wave suspensions were quantitatively analyzed. More than ten commercial products were fluorescently labeled, while the separation of the derived analytes could be accomplished within 20 seconds.

The achieved findings of this work, along with perspectives for future applications in this field are discussed in chapter 6. Although microchip separations have not yet fully reached the ruggedness and reliability of other more traditional separation methods, they clearly have the potential to increase the speed and efficiency of separations to a great extent. While still not many quantitative on-chip determinations can be found in literature, this work shows the successful application of the newly developed wavelength-resolved detection system to the quantitative determination of real samples.

Samenvatting

Dit proefschrift beschrijft de ontwikkeling en toepassing van een nieuwe op CCD gebaseerde fluorescentiedetector met golflengteresolutie voor microchip scheidingen.

In de laatste jaren is miniaturisatie een van de hoofdtrends in de ontwikkeling van nieuwe analytische scheidingssystemen. Aangezien de bewerkte mon-sterhoeveelheden en detectievolumes op microchips kleiner en kleiner zijn geworden, is de noodzaak voor hoge-prestatie dectectiesystemen groter dan ooit. Toegepaste detectiemethoden moeten secuur aangepast worden aan de kleine dimensies en de hoge snelheid van microchipscheidingen.

Hoofdstuk 2 geeft een overzicht van de recente ontwikkelingen op het gebied van optische detectiemethoden voor microchipscheidingen en belicht nieuwe benaderingen voor hoge-prestatie detectetietechnieken.

UV/vis spectroscopie, als een van de traditionele methoden voor detectie in vloeistofscheidingen, is slechts van ondergeschikt belang in microchip CE, aangezien de beschikbare optische weglengtes zeer klein zijn en alleen lage gevoeligheid toestaan. Fluorescentiedetectie daarentegen kan eenvoudig aangepast worden aan microchipformaat, wanneer sterk gefocusseerd excitatielicht wordt gebruikt. Uitstekende resultaten zijn bereikt met laser geïnduceerde fluorescentie (LIF), omdat de uiterst coherente laserstraal

makkelijk te focusseren is op kleine detectievolumina, resulterend in hoge bestraling. De combinatie met een zeer gevoelige detector, zoals een fotovermenigvuldigingsbuis (PMT), geeft de laagst mogelijke detectielimieten die momenteel haalbaar zijn. Desondanks wordt weinig tot geen chemische and structurele informatie van de te bepalen verbinding verkregen.

Om de hoeveelheid informatie van een microchip capillaire electroforese (MCE) scheiding te verhogen, is dit werk erop gericht om de aantrekkelijke benadering om spectrale informatie toe te voegen aan de fluorescentie detectie door middel van het geëmitteerde licht te breken, waarmee het mogelijk wordt gemaakt om de volledige on-line emissiespectra op te nemen. Bestaande uit een fluorescentiemicroscoop met een excitatiebron gebaseerd op een regelbare lamp, een spectrograaf en een versterkte CCD-camera, vormt deze opstelling een flexibel en vermogend detectorsysteem, goed aangepast aan MCE scheidingen. De detectie van het gedispergeerde emissielicht levert electroferogrammen met golflengteresolutie. Vergelijkbaar aan een diode-array detector in UV/vis absorptie levert de detectie van volledige emissiespectra gedurende de analyse waardevolle informatie betreffende de te bepalen verbindingen.

Hoofdstuk 3 richt zich op de ontwikkeling van de detectoropbouw en beschrijft de implementatie van de onderdelen in detail. Het electroforetische scheiding van drie rhodamine kleurstoffen met verschillende fluorescentie-eigenschappen toont als modelsysteem prestatie van het instrument. Submicromolaire concentraties zijn gedetecteerd en de toegevoegde

dimensie van informatie verkregen middels golflengte-resolutie wordt gebruikt om de pieken toe te kennen en voor de piek-zuiverheidsbepaling. Gebruik makend van een dergelijke evaluatiemethode kan verborgen co-elutie in kaart worden gebracht.

Aangezien kwantitatieve en reproduceerbaarheidsanalyses op microchip nog steeds een uitdaging zijn, wordt de toepasbaarheid van het nieuw ontwikkelde detectorsysteem aan monsters vanuit de praktijk beschreven in hoofdstuk 4. Dit deel van het proefschrift richt zich op de bepaling van de hoeveelheid taurine in dranken. Meer dan tien verschillende energie-, sport- en andere taurinehoudende dranken zijn geanalyseerd middels MCE. De snelste scheiding van fluorescent-gelabelde taurinederivaten die tot nu toe bekend is (12 seconden) kon bereikt worden. Met goede lineariteit over een breed concentratiebereik is het detectiesysteem met golflengteresolutie succesvol toegepast en gevalideerd met behulp van een onafhankelijke HPLC methode.

Hoofdstuk 5 behandelt de bepaling van thiolische verbindingen in consumentproducten. De actieve ingrediënten van ontharingscrème en koude-golfsuspensies zijn kwalitatief geanalyseerd. Meer dan tien commerciële producten zijn fluorescent gelabeld en de scheiding van de respectievelijke derivaten kon binnen 20 seconden bereikt worden.

De behaalde resultaten van dit werk samen met de perspectieven voor toekomstige toepassingen op dit gebied worden beschreven in hoofdstuk 6. Hoewel microchipscheidingen nog niet de volledige robuustheid en

betrouwbaarheid hebben van meer traditionele scheidingsmethoden, hebben ze duidelijk het vermogen om de snelheid en efficiëntie van scheidingen behoorlijk te verhogen. Waar er in de literatuur nog maar weinig kwantitatieve op-chip bepalingen beschikbaar zijn, laat dit werk zien hoe het nieuw ontwikkelde detectiesysteem met golflengteresolutie succesvol toepasbaar is voor de kwantitatieve bepaling van reële monsters.

Acknowledgements

Furthermore I would like to thank all the Dutch colleagues who welcomed us in the Netherlands. I thank Annemarie Montanaro-Christenhusz and Martijn Heuven for all their help in the lab and Nancy Heijnekamp for knowing her own special ways to magically speed up the delivery process of urgently needed chemicals.

I also thank the Fonds der Chemischen Industrie (Frankfurt/Main, Germany) for the financial support of my work with a PhD. student grant.

Nicht zuletzt möchte ich auch meinen Eltern danken, da diese Arbeit den Abschluss einer Ausbildung darstellt, die nur durch ihre andauernde und bedingungslose Unterstützung möglich wurde.

Mein besonderer Dank gilt Tanja, für ihren Beistand und die nötige Motivation besonders auch in stressigen Lebenslagen.

Curriculum Vitae

Personal Details

Name: Sebastian Götz

Date of Birth: July 27th,1976

Place of Birth: Soest, Germany

Nationality: German

Education

1983-1987   Georgs-Grundschule in Soest, Germany

1987-1996   Aldegrever-Gymnasium in Soest, Germany,

                Graduation in May 1996

1996-1997   Military Service

1997-2002   Studies of Chemistry at the Westfälische Wilhelms-
                Universität Münster, Germany

2000-2002   Scholarship of the Studienstiftung des Deutschen Volkes,
                (Bonn, Germany)

March 2002   Graduation with the thesis entitled "MALDI-TOF-MS zur
                Bestimmung des Markierungsgrades von Proteinen"
                (practical work performed at the University of Twente
                (Enschede, The Netherlands) with Prof. Dr. Uwe Karst)

April 2002	Begin of dissertation in Analytical Chemistry at the University of Twente (Enschede, The Netherlands) with Prof. Dr. Uwe Karst
2002-2004	Scholarship of the Fonds der Chemischen Industrie (Frankfurt/Main, Germany)

List of Publications

Original Papers

Liquid Chromatography with On-Line Electrochemical Derivatization and Fluorescence Detection for the Determination of Phenols

Meyer J, Liesener A, Götz S, Hayen H, Karst U (2003) Anal Chem 75:922-926

Recent Developments in Optical Detection Methods for Microchip Separations

Götz S, Karst U (2006), submitted for publication

Wavelength-Resolved Fluorescence Detector for Microchip Separations

Götz S, Karst U (2006), submitted for publication

Training and Testing Explosive Detection Dogs in Detecting TATP

Schoon A, Götz S, Heuven M, Vogel M, Karst U (2006) Forensic Sci Commun, accepted for publication

Quantitative On-Chip Determination of Taurine in Energy and Sports Drinks

Götz S, Revermann T, Karst U (2006), submitted for publication

Quantitative Analysis of Thiols in Consumer Products on a Microfluidic Capillary Electrophoresis Chip with Fluorescence Detection

Revermann T, Götz S, Karst U (2006), submitted for publication

Other Publications:

Trends in der Analytik

Karst U, Götz S (2004) Analytica Pro 8-10

Chemical Analysis in Twente

Karst U, Götz S (2004) G.I.T. Laboratory Journal 4:2-3

Oral Presentations:

Multidimensional Fluorescence Detection for Capillary and On-Chip Separations

PITTCON (Pittsburgh Conference on Analytical Chemistry and Applied Spectroscopy), 2003, Orlando, USA

CCD-Basierte Fluoreszenzdetektion für Kapillar- und On-Chip-Trennverfahren

Incom (International Symposium on Instrumentalized Analytical Chemistry and Computer Technology), 2003, Düsseldorf, Germany

Mehrdimensionale Fluoreszenzdetektion für Flüssigchromatographische und Elektrophoretische Trennverfahren

Jahrestagung-Chemie der Gesellschaft der Deutschen Chemiker (GDCh), 2003, München, Germany

Multidimensionale Fluoreszenzdetektion für Kapillar- und On-Chip-Trennverfahren

Doktoranden-Seminar des Arbeitskreises "Separation Sciences" der GDCh, 2004, Kloster Banz, Germany

Liquid-Phase Separations with CCD-Based Spectrally Resolved On-Line Fluorescence Detection

HTC-8 (Hyphenated Techniques in Chromatography), 2004, Brugge, Belgium

Multidimensional Fluorescence Detection for Capillary and On-Chip Separations

ISC (International Symposium on Chromatography), 2004, Paris, France

Multidimensional Fluorescence Detection for Fast On-Chip Separations

PITTCON (Pittsburgh Conference on Analytical Chemistry and Applied Spectroscopy), 2005, Orlando, USA

Wellenlängenaufgelöste Fluoreszenzdetektion für Elektrophoretische (On-Chip)-Trennverfahren

ANAKON, 2005, Regensburg, Germany